PHILOSOPHICAL TRANSACTIONS OF THE ROYAL SOCIETY A MATHEMATICAL, PHYSICAL & ENGINEERING SCIENCES

Electron Collision Studies with Trapped Positive Ions

F. A. Baker and J. B. Hasted

Phil. Trans. R. Soc. Lond. A 1966 **261**, 33-65
doi: 10.1098/rsta.1966.0057

ELECTRON COLLISION STUDIES WITH TRAPPED POSITIVE IONS

By F. A. BAKER
Institut Battelle, Geneva
and J. B. HASTED
University College London

(*Communicated by Sir Harrie Massey, F.R.S.—Received 28 October 1965—Revised 24 January 1966*)

CONTENTS

Positive ions have been trapped for periods of *ca.* 100 μs within the space charge of a magnetically confined electron beam, ionized by this beam and detected mass-spectrometrically. The theory of the trap is developed and compared at many points with experiment. Cross section functions are given for the ionization of Ne^+, Ar^+, Kr^+, Xe^+, and the dissociation of CO^+ by electrons; the ionization of Ne_2^+ and CO^+ by electrons is also investigated. From measurements of fragment ion currents CH_2^+, CH^+ from methane, it is shown that the dissociation of CH_4^+ by electrons can contribute unwanted effects interfering with the appearance potential of the fragment ion. Effects due to excitation of ions by electrons are observed in the noble gases.

Introduction

The ionization and excitation of positive ions by electrons have been studied experimentally by crossed beam techniques (Dolder, Harrison & Thonemann 1961, 1963; Latypov, Kupriyanov & Tunitskii 1964; Kupriyanov & Latypov 1963) and by theoretical means (Burgess 1961; Drawin 1961). A different experimental approach, expected to enjoy certain advantages, is that of causing an electron beam to pass through a region in which positive ions are held trapped by an electric or magnetic field. The space charge of the electron beam can conveniently be utilized to form the trapping field. This paper discusses the

theory of such experiments and reports the results of measurements on the ionization of Ne^+, Ar^+, Kr^+, Xe^+, Ne_2^+, CO^+, and the dissociation of CO^+ and CH_4^+ by low energy electrons.† Certain other collision processes can also be investigated, and proposals are made for more extended study.

1. Potential distribution in the electron space-charge trap

The space charge of an electron beam forms an electric potential well or 'ion trap' within the beam. Although the presence of a confining magnetic field is by no means essential to trap formation, we have chosen to study the case in which the electron beam flows along the lines of force of a steady magnetic field (1830 G), the electrons being confined to helical paths as in the mass spectrometer source described by Bleakney (1929, 1932) and Nier (1940, 1947). This simple electrode system (figure 1 (*a*, *b*)), obtained by making only minor modifications to a small commercially available 180° mass spectrometer (British A.E.I., MS 10), serves as a good starting point for electron collision studies with trapped ions.

(*a*) *Transverse to the electron beam*

For a cylindrical electron beam of radius a carrying total current I_e, and confined to helical paths by a magnetic field of infinite extent and intensity in a region free of electric field, the charge density ρ can be taken to be independent of radius variable r; it is given in m.k.s. units by

$$\rho = \frac{-I_e}{\pi a^2 \sqrt{(2\eta V)}}, \tag{1}$$

where η is the electron charge/mass ratio and V the electric potential with respect to the cathode. Following the treatment of Pierce (1949) Poisson's equation is written

$$\frac{1}{r}\frac{\partial}{\partial r}\left(r\frac{\partial V}{\partial r}\right) = \frac{I_e}{n\epsilon_0 a^2 \sqrt{(2\eta V)}}. \tag{2}$$

This equation has a special solution

$$V = \left(\frac{9}{16\pi\epsilon_0\sqrt{(2\eta)}}\right)^{\frac{2}{3}}\left(\frac{r}{a}\right)^{\frac{4}{3}} I_e^{\frac{2}{3}}, \tag{3}$$

in which $V = 0$ on the cylinder axis and a virtual cathode is formed. In the presence of sufficient positive ions this charge configuration will pass discontinuously into the 'real cathode' solution; experimental studies of this situation have been made by Lloyd (1965). For the 'real cathode' solution, appropriate to the less intense beams of the present experiments, one introduces a variable

$$\phi = V/V_0, \tag{4}$$

where V_0 is the value of V on the beam axis, and is taken as equal to the electron accelerating voltage V_e. Defining a reduced radius ρ, we have

$$\rho = r\left(\frac{I_e}{V_0^{\frac{3}{2}}\pi\epsilon_0 a^2\sqrt{(2\eta)}}\right)^{\frac{1}{2}}. \tag{5}$$

Equation (2) becomes

$$\frac{1}{\rho}\frac{\partial}{\partial\rho}\frac{\partial\phi}{\partial\rho} = \phi^{-\frac{1}{2}} \tag{6}$$

† Since presenting this material at the Fourth International Conference on the Physics of Electronic and Atomic Collisions, the authors have become aware of similar ideas advanced by Dr C. Hutchinson of the Argonne National Laboratory, U.S.A.

which must be solved for boundary conditions $\rho = 0$, $\phi = 1$ and $\partial\phi/\partial\rho = 0$. An iterative method has been employed on the London University Atlas computer, to obtain a numerical solution. For $\rho \leqslant 0{\cdot}32$, the relatively low intensities of the present experiments, an acceptable approximate solution is

$$\rho^2 \simeq 4(\phi - 1). \tag{7}$$

Equations (4), (5) and (7) lead immediately to

$$V = \frac{I_e r^2}{4V_0^{\frac{1}{2}} \pi\epsilon_0 a^2 \sqrt{(2\eta)}} + V_0 = Kr^2 + V_0. \tag{8}$$

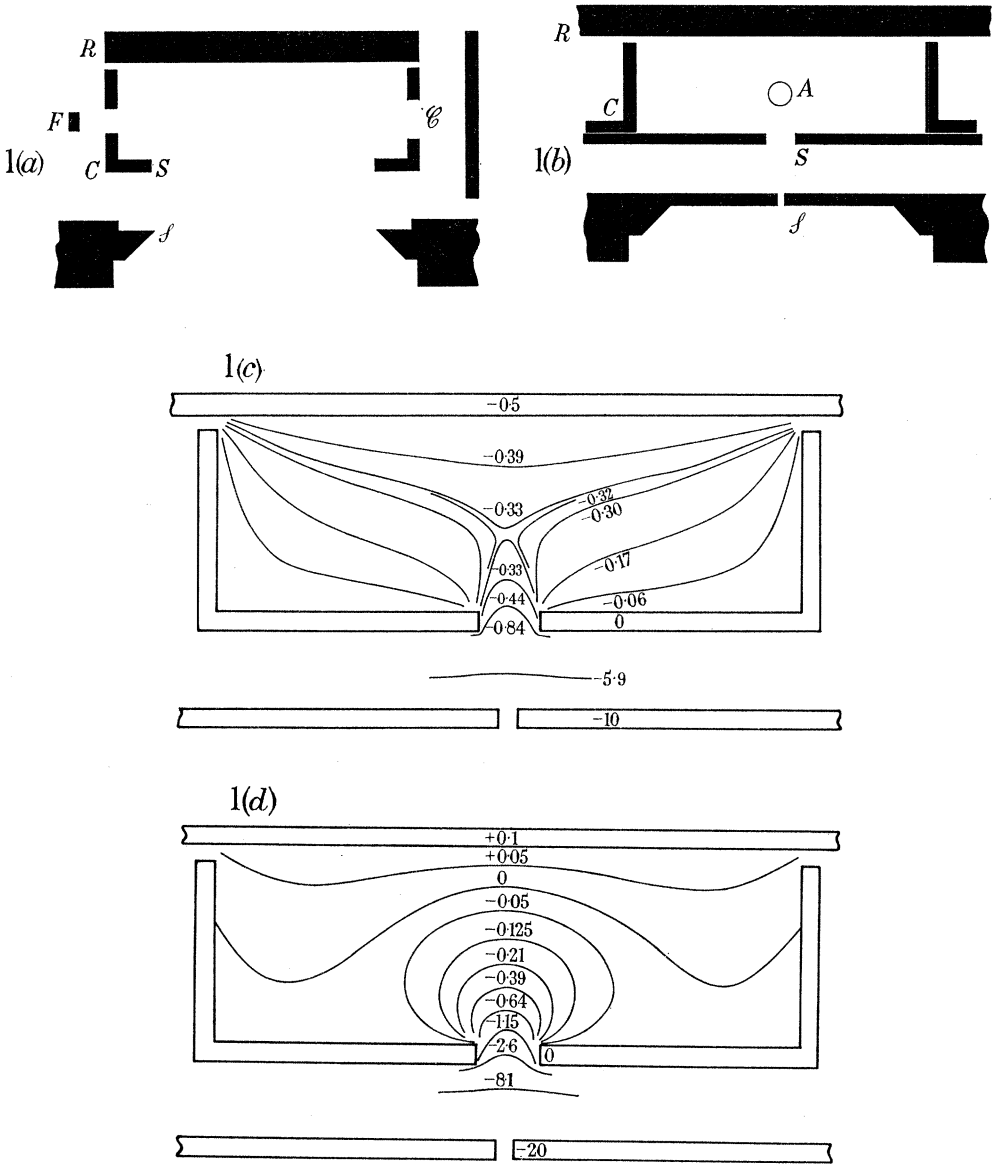

FIGURE 1. Views, to scale, of collision chamber C for electron impact.

(a) At right angles to magnetic field.
(b, c, d) Along magnetic field and electron beam.
(c, d) Equipotentials shown as full lines.
(c) $V_{\mathscr{S}} = -10$ V, $V_R = -0{\cdot}5$ V, $V_C = 0$V.
(d) $V_{\mathscr{S}} = -20$ V, $V_R = +0{\cdot}1$ V, $V_C = 0$V.
A, orifice for definition of electron beam (diameter 1 mm), R, repeller, F, filament, S, extraction slit, $\mathscr{S}$, analysis slit, $\mathscr{C}$, electron collector.

For $I_e = 50\,\mu\text{A}$, $V_0 \simeq 30\,\text{V}$, $a = 0{\cdot}5\,\text{mm}$, $K = 55{\cdot}2\,\text{V}^{-1}\,\text{cm}^{-2}$, so that cylindrical potential traps of depth $> 0{\cdot}1\,\text{V}$ are readily obtained. A unique ratio $I_e/V_0^{\frac{1}{2}}$ will yield a unique $V(r)$; to achieve an ion trap of invariant properties, it would be necessary to scale the current appropriately when the electron accelerating potential V_e is varied. But since the range of its variation is comparatively small in the present cross section function measurements, the application of 'current scaling' has not been made extensively, and has not yet been found to affect the situation seriously (see §§ 2 (*a*), 4 (*g*)).

Broadly speaking, ion trapping will take place when the trap depth $V_T = Ka^2$ exceeds the kinetic energy of the ion at formation; this is often approximately $\frac{3}{2}kT \simeq 0{\cdot}04\,\text{eV}$.

In the mass spectrometer source there is usually appreciable electric field transverse to the confined electron beam, arising from

(i) A potential V_R sometimes applied to a 'repeller electrode' situated on the opposite side of the beam to the ion extraction slit.

(ii) The field that penetrates through the ion extraction slit from the strongly negative region outside it.

Two situations may be distinguished, corresponding to positive and negative repeller potentials; contrasting potential configurations, obtained for our source by measurements with resistive paper, are shown in figure 1 (*c*, *d*).

The influence of the electron beam upon the transverse potential is small, because there is negligible transverse conductivity due to the electrons, which are strongly confined axially by the magnetic field. In contrast, the influence of the transverse field upon the space-charge trap configuration is considerable. A fair approximation would be to consider the circumference of the beam to be situated in an undisturbed electric field, whilst within the beam, along each radius, the distribution of potential remains that of the appropriate solution of equation (8); thus the beam is not regarded as being affected by the external field except insofar as the circumferential potential is caused to vary. This has the effect of distorting the radially symmetrical trap in the manner of figure 2, which shows equipotentials calculated for some uniform variations of potential across the beam circumference.

Within the closed loops of figure 2, positive ions will be held in a radial trap, and will undergo approximately radial but precessing oscillations; outside this area positive ions will only undergo a small number of oscillations, escaping from the circumference of the beam when the appropriate azimuthal angle is reached. The 'trap area' will be denoted by A_T and the 'free area' by A_F. It is apparent that increase of transverse field increases A_F at the expense of A_T.

In the present experiments we attempt to maximize A_T, so that collisions between electrons and trapped ions will yield the maximum current of doubly charged ions. For heavy atoms whose extraction field is small, this will be achieved with repeller potential V_R very close to zero, but for light atoms with larger extraction field, a good radially symmetrical trap is impossible to achieve; however a strongly negative V_R maximizes doubly charged ion current. An ideal trap would require a pulsed extraction potential and zero repeller potential.

For a certain negative repeller potential the 'neutral region' of potential (figure 1 (*c*)), where repeller and extraction fields balance to produce vanishing electric field, will coincide with the electron beam. In this case the transverse field will usually be too small to overcome the trapping potential, so that radial trapping of ions can occur. There will also be a certain

positive value of repeller potential (figure 1 (*d*)) for which the electron beam passes through an equipotential identical with the walls of the impact chamber. Although in this situation there is a field transverse to the beam, trapping along the axis of the beam (see § 1 (*b*)) is not inhibited, and, provided that the radial trapping field is sufficiently intense, some ions will remain within the beam. Thus the characteristic form of the trapped ion current repeller function will be: one sharp peak at a negative value of V_R, approximately inversely proportional to extraction potential V_x (hence to mass number, since in this instrument $V_x = 4150/m_+$, with ion mass number m_+ in a.m.u.): and one smaller peak at a positive V_R, also inversely proportional to mass number; in practice the latter is only within the experimental range of V_R for heavy ions. These are the characteristics of figure 6.

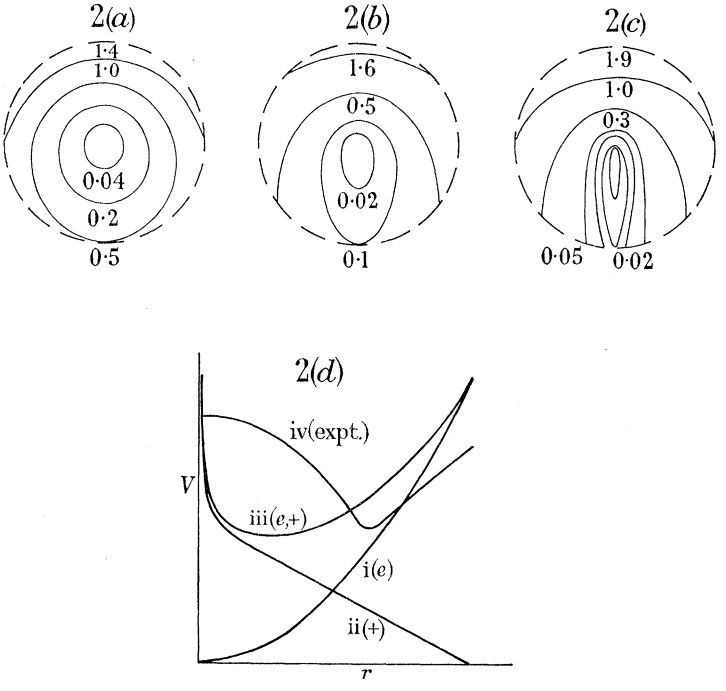

FIGURE 2. Distortion of circular equipotential lines of a radially symmetrical space-charge trap when a uniform transverse field is applied. Depth of undistorted radial trap (*a*, *b*, *c*,) 1 V; transverse potential drop across diameter: (*a*) 1 V, (*b*) 1·9 V, (*c*) 1·99 V. Numbers denote potentials in volts. (*d*) Typical radial potential functions: i, due to electrons only (equation (8)); ii, due to ions only (equation (17)); iii, sum of i and ii; iv, trial function used for calculation of electron energy distribution.

(*b*) *Along the electron beam*

It is necessary for ion trapping that there be a potential minimum along the axis of the electron beam.

Calculations are available (Lloyd 1965) of the potential distribution $V(z)$ along a z axis one-dimensional beam passing between two equipotential surfaces separated by a distance l and held at a potential V_l. For current density J, in a magnetic field of infinite extent and intensity,

$$\frac{Jz(z-l)}{\epsilon_0\sqrt{(2\eta)}} = 4[(V_l^{\frac{1}{2}} - V_m^{\frac{1}{2}})^{\frac{1}{2}} V_m^{\frac{1}{2}} - (V^{\frac{1}{2}} - V_m^{\frac{1}{2}})^{\frac{1}{2}} V_m^{\frac{1}{2}} + \tfrac{1}{3}(V_l^{\frac{1}{2}} - V_m^{\frac{1}{2}})^{\frac{3}{2}} - \tfrac{1}{3}(V^{\frac{1}{2}} - V_m^{\frac{1}{2}})^{\frac{3}{2}}]^2; \qquad (9)$$

at $z = \frac{1}{2}l$ there is a potential minimum of depth V_m. Owing to the limited nature of this model the potential minima of equation (9) are much deeper than those observed in Lloyd's experiments, so that for a plausible estimate of longitudinal field by means of equation (9), the real current density must, according to Lloyd, be multiplied by a factor of 0·01. Thus in the present studies $l = 1$ cm, $I_e = 50\ \mu$A, $V_l = 30$ V, and the longitudinal trapping potential $V_l - V_m$ is little more than 1 V.

If the conditions for extraction field balancing by repeller potential are not met, the ion extraction potential can lead to field penetration sufficient to destroy the trapping field, or to confine it to a very small volume.

Field penetration from the cathode region and effects of secondary electrons emitted by the electron collector can also affect the longitudinal potential well.

In the present experiments the longitudinal trapping field is more powerful than the radial trapping field; escape from it is more difficult, so that ions become concentrated in the region above the extraction slit. Using the analogy of a ball rolling on a concave potential surface, the ions in the trap would be imagined as rolling on the inside surface of a discus or puck, rather than in a groove.

(*c*) *Influence of slow electrons and positive ions on the radial potential well*

We now consider the effect of the gradual creation (by collisions) of positive ions and slow electrons upon the radial configuration of the potential trap.

Slow electrons formed by ionization are confined by the magnetic field to helical paths, whose radius will be neglected; the helical axes are longitudinal. The extra negative charge density so produced is independent of radius variable, and may be treated by the method applied to beam electrons, leading to an equation exactly similar to (8). In this equation one may use for the slow electrons a value of I_e given by equations (14) and (15); the appropriate value of V_0 is thermal (0·039 eV at $T = 300$ °K), plus corrections from longitudinal potential variation. Under the conditions of the present experiments, the slow electrons do not change the form of the radial potential function at all, and only change its magnitude by a small amount.

We now show that the effect of positive ion creation is to transform the trap cross section from circular to annular without the creation of any instability. If we postulate a continuous leakage of ions from the radial trap, balancing the continuous formation of ions by electron-gas collisions, then the radial trap area will achieve an equilibrium value.†

Consider a positive ion formed with zero kinetic energy at a distance r_0 from the beam axis, within a radially symmetrical potential well of configuration

$$V(r) = Kr^2, \tag{10}$$

with K given by equation (8). Neglecting collisions, the ion will execute radial oscillations, with energy equation

$$(r_0 - r)\,\eta_+ \frac{\mathrm{d}V}{\mathrm{d}r} = \tfrac{1}{2}v_r^2, \tag{11}$$

† In the absence of magnetic field, the situation has been considered by Hartnagel (1965).

PHILOSOPHICAL TRANSACTIONS OF THE ROYAL SOCIETY A MATHEMATICAL, PHYSICAL & ENGINEERING SCIENCES

where η_+ is its charge/mass ratio and v_r its radial velocity. For ions formed in the beam, the radial density function is written as the inverse of the velocity distribution function

$$\frac{n_+}{\bar{n}_+} = \frac{1}{a}\int_r^a r_0 v_r^{-1}\,\mathrm{d}r_0 \tag{12}$$

which, with the aid of (10) and (11), becomes

$$\frac{n_+}{\bar{n}_+} = \frac{1}{3a\sqrt{(\eta_+ K)}}\,\frac{(a+2r)\,(a-r)^{\frac{1}{2}}}{r^{\frac{1}{2}}}. \tag{13}$$

The space averaged density $\bar{n}_+$ can be written

$$\bar{n}_+ = n_e v_e n_0 \sigma_i t, \tag{14}$$

in which n_0 is the gas number density, σ_i the electron-atom ionization cross section, and t the time over which we consider the buildup of ion density; the uniform electron number density n_e and velocity v_e are related numerically to the current I_e

$$n_e v_e = I_e \mathscr{C}/\mathscr{A} \tag{15}$$

where $\mathscr{C} = 6{\cdot}24\times 10^{18}$ coulomb^{-1} and $\mathscr{A}$ is the area of the cross section of the beam (Gaussian units). This is a more convenient form than equation (1) and will be used henceforward.

Equations (13) and (14) may now be combined with Poisson's equation for the positive ions,

$$\frac{1}{r}\frac{\partial}{\partial r}\left(r\frac{\partial V_+}{\partial r}\right) = \frac{n_+ e}{\epsilon_0}, \tag{16}$$

where $\mathscr{C}$ is the ionic charge and $V_+(r)$ the potential function resulting from ions alone. Although it is unsatisfactory simply to add the electron and positive ion radial potential functions as though there were no coupling between them, some idea of the neutralization of the radial trap by the positive ions may be obtained by this procedure. Using the arbitrary boundary condition $\mathrm{d}V/\mathrm{d}r = -K$ at $r = \frac{1}{2}a$, a solution for $V_+(r)$ is obtained

$$-V_+ = 3C(2r^5 - 3ar^3) + A\ln r + B, \tag{17}$$

where

$$C = \frac{e\bar{n}_+}{3\epsilon_0 a\sqrt{(\eta_+ K)}},$$

$$A = -\tfrac{1}{2}Ka + 3Ca\{(\tfrac{1}{2}a)^3 - \tfrac{2}{5}(\tfrac{1}{2}a)^5\},$$

$$B = 3C(3a^4 - 2a^5) - A\ln a.$$

We see from the form of this equation (figure 2 (*d*)) that V_+ is infinite at $r = 0$, but is zero and varies comparatively slowly at $r = a$. Thus the positive ion space charge dominates only in the centre of the beam, and transforms the trap cross section from circular to annular. When $V(r)$ (equation (8)) is added to $V_+(r)$ (equation (17)), the potential minimum is found at a value of r intermediate between 0 and a (figure 2 (*d*)); provided that the experimental pressures do not exceed 10^{-5} torr, and that the time t in equation (14) is of the order of the 'trapping times' discussed below, we find that $V_+(r)$ is negligible compared with $V_e(r)$ (equation 8) for $r = 0{\cdot}9a$.

In this situation we can treat the leakage of ions from the trap by assuming a 'rate of extraction', $\bar{n}_+\kappa_1$ ions per second, proportional to the space average $\bar{n}_+$ of singly charged ion density. The constant of proportionality κ_1, or singly charged ion extraction rate constant,

is the inverse of the mean trapping time τ_1. We shall assume in §§ 2 (a, b) that κ_1 is independent of gas pressure. This can only be so if the circumference of the trap, from which the leakage takes place, is largely unaffected by the positive ion mean density, given by equation (14). These are the conditions we have shown above to be applicable. For the calculation of leakage rate we therefore assume that the circumferential trap potential $V(a)$ is equal to the electron contribution $V(a)$ given by equation (8).

An ion at the maximum amplitude of its oscillation will leave the trap when its thermal energy exceeds the trapping potential ΔV_T. The condition

$$\Delta V_T \leqslant \tfrac{3}{2}kT \tag{18}$$

applies for values of r greater than an extraction radius r_e, where

$$\Delta V_T = Ka^2 - Kr_e^2. \tag{19}$$

If there were no field an ion would spend in the trap an average time

$$t^* = a/2\bar{v}_+, \tag{20}$$

where

$$\bar{v}_+ = \sqrt{(2kT/m_+)}. \tag{21}$$

But since there is a space-charge field, a trapped ion does not pass outward until after a time τ_1. We suppose that when the ions are in equilibrium under the action of the space-charge field, the ratio of extraction region ions to total trap ions is

$$\frac{t^*}{\tau_1} = \int_{r_e}^{a} \frac{(a+2r)\,(a-r)^{\frac{1}{2}}}{r^{\frac{1}{2}}}\,\mathrm{d}r \Big/ \int_0^a \frac{(a+2r)\,(a-r)^{\frac{1}{2}}}{r^{\frac{1}{2}}}\,\mathrm{d}r$$

$$= 1 - \frac{8}{10\pi}\left\{\sin\left(2\arcsin\sqrt{\frac{r_e}{a}}\right) + 2\arcsin\sqrt{\frac{r_e}{a}}\right\} + \frac{1}{10\pi}\left\{\sin\left(4\arcsin\sqrt{\frac{r_e}{a}}\right) - 4\arcsin\sqrt{\frac{r_e}{a}}\right\}. \tag{22}$$

Equations (18) to (22) ((18) applying as an equality) lead to trapping times which will under suitable conditions dominate the collisional extraction mechanisms to be considered in § 2 (b). For example, for krypton ions in a trap with $I_e = 50\ \mu\mathrm{A}$, $V_0 \simeq 30\ \mathrm{V}$, $a = 0{\cdot}5\ \mathrm{mm}$, we infer from the data that $\tau_1 \sim 10^{-4}\,\mathrm{s}$ (see §§ 2 (a, c)).

Two criticisms may be made of this approach:

1. The actual radial electric field in the beam should be given by a self-consistent expression, not merely a sum of two self-consistent fields. Thus in the field defined by $V(r)+V_+(r)$ the ions will satisfy a different equation of motion from (11), so that the calculation of $V_+(r)$ should be modified accordingly, and equations (11) to (22) iterated.

2. Neglect of momentum exchange between atom and electron is not always justified.

However, the radial potential function may be deduced from the observed electron energy distribution in the collision region. As computed from the second differential of the helium ionization function, the distribution has energy wings, shown in figure 3 (a) (inset). The energy distribution may be considered as a convolution of the thermal plus longitudinal distribution $n_{et}(V)$ with the radial distribution $n_{er}(V)$

$$n_e(V) = n_{et}(V)\,n_{er}(V). \tag{22a}$$

Writing the radial distribution in the form $r = f(V)$, we have $\mathrm{d}r = f'(V)\,\mathrm{d}V$, so that

$$n_{er}(V) = 2\frac{I_e\mathscr{C}}{a^2} f(V)f'(V)\,\mathrm{d}V. \tag{22b}$$

The dotted curve in figure 3 (*a*) (inset) is now shown to be a convolution of a hypothetical square $n_{et}(V)$ (chosen for ease of calculation) with an $n_{er}(V)$ calculated from equation (22*b*) using the trial $V(r)$ shown as curve iv in figure 2 (*d*). We may regard this $V(r)$ as a realistic function deduced from the experimental energy distribution; it is at variance with the function deduced from equations (8) and (17), but at least it exhibits a potential minimum, characteristic of an ion trap of annular cross section. The longitudinal potential variation is neglected.

2. Kinetics of the ion trap

(*a*) *No ion-gas collisions within the ion trap*

Consider first the consequences of the assumption that an ion spends, on the average, a trapping period τ_n (for n-charged ions) confined within the 'trap area' A_T. Secondary processes occurring in the 'free area' A_F are neglected, since the time spent there, t_f, is small compared with the trapping time (see § 4 (*c*)). No assumptions are made, as yet, about the mechanism of extraction, but in the absence of collisional processes the time τ_n is equal to the inverse of the loss rate constant κ_n. During the time τ_1 the singly charged ion population of the beam passes out of the trap and is replaced by an equal population. The singly charged ion current measured in the mass spectrometer is therefore:

$$I_+ = \mathscr{E} n_+ l \left(\frac{A_T}{\tau_1} + \frac{A_F}{t_f}\right) \quad \text{(in Gaussian units)}, \tag{23}$$

where $\mathscr{E}$ is the efficiency with which the mass spectrometer collects ions issuing from the working length l of the electron beam. The symbols n denote space averaged species densities (cm^{-3}) throughout; the space averages of singly charged ion density in the trap and free areas are assumed the same. For doubly charged ions

$$I_{2+} = \frac{\mathscr{E} n_{2+}}{\tau_2} A_T l \tag{24}$$

since we neglect the formation of doubly charged ions by single processes in the free area. As in equation (15)

$$n_+ = n_e n_0 \sigma_i \tau_1 v_e \tag{25}$$

and

$$n_{2+} = n_e n_+ \sigma_{2i} \tau_2 v_e, \tag{26}$$

where σ_i and σ_{2i} are respectively the cross sections for formation by electron impact of singly charged ions from neutrals and doubly charged ions from singly charged ions. In the present studies electrons are not permitted to possess sufficient energy eV_e to exceed the threshold for the production of doubly charged ions from neutrals; also, inelastic heavy particle collisions are neglected. We have immediately

$$I_+ = \mathscr{E} n_e l v_e n_0 \sigma_i \left(\frac{A_T}{\tau_1} + \frac{A_F}{t_f}\right) \tau_1, \tag{27}$$

$$I_{2+} = \mathscr{E} n_e^2 l v_e^2 n_0 \sigma_i \sigma_{2i} A_T, \tag{28}$$

and using equation (15),

$$\frac{I_{2+}}{I_+} = \frac{I_e \mathscr{C} \sigma_{2i}}{\mathscr{A}} \left(\frac{A_T/\tau_1}{A_T/\tau_1 + A_F/t_f}\right) = \frac{I_e \mathscr{C} \sigma_{2i} c_T}{\mathscr{A}}, \tag{29}$$

in which we define ϵ_T, the trap efficiency, and note in passing that

$$\tau_1 = \frac{A_T}{A_F}\left(\frac{1-\epsilon_T}{\epsilon_T}\right) t_f. \tag{30}$$

Since ϵ_T is relatively insensitive to V_e (although strictly a current scaling procedure, as outlined in § 1 (*a*), should be adopted), equation (25) can be applied to measurements of I_{2+} and I_+, at a single value of I_e, V_r and pressure p to yield the required cross section function $\sigma_{2i}(V_e)$. And since ϵ_T can only be calculated from theory in the correct order of magnitude (even this involves many assumptions), the cross section σ_{2i} is relative, and must at present be normalized to existing data.

Provided that σ_{2i} is known independently the efficiency ϵ_T may be calculated from the data. In our experiments the efficiencies were at first very small ($\sim 0{\cdot}001$), but methods have now been found of raising ϵ_T to values as high as 0·1. For $\epsilon_T \ll 1$,

$$\epsilon_T \simeq A_T t_f / A_F \tau_1, \tag{31}$$

and since the ratio t_f/τ_1 may only be calculated within an order of magnitude from equations (17) to (22), the ratio A_T/A_F can only be deduced to this accuracy. Nevertheless, a well balanced trap should possess at least as much trap as free area, and in § 4 (*c*) we will consider the consequences of taking $A_T/A_F \sim 1$.

We note from equation (28) that $I_{2+} \propto I_e^2$. When this condition is achieved experimentally, A_T is inferred to be invariant with I_e, hence with electron energy eV_e, so that current scaling is unnecessary. A more rigid test is that $I_+ \propto I_e$ (equation (27)), which implies that $A_T + A_F \tau_1/t_f$ is invariant with eV_e. In general these conditions have been met in our experiments, but departures from them indicate that the ion trap is sensitive to V_e, and will not yield perfect cross section functions without a scaling procedure.

However the variation of I_{2+} with gas pressure is incorrectly interpreted by equation (28), so that the kinetics of collisional processes in the trap must be discussed; we infer from these variations the relative importance of different types of inelastic collision and elastic collisional extraction.

(*b*) *Kinetics of collisions within the ion trap*

While the processes leading to the formation of ions in the trap area may readily be understood on the conventional background of collision physics, the processes leading to extraction cannot easily be deduced from first principles, and must therefore be inferred from the variation of measured ion currents with pressure and electron current. The results of our experiments may be summarized as follows:

$I_+ \propto p$ over three orders of magnitude (figure 7); but in some cases a more accurate representation is $I_+ \propto Ap/(Bp+C)$; $I_+ \propto I_e$ at low currents (figure 9), but a polynomial would be a better representation; at high currents I_+ (I_e) can actually pass through a maximum and fall rapidly. I_{2+} (figure 8) is in general invariant with pressure in the limit of high p, being represented in the range 10^{-5} to 5×10^{-7} torr by $I_{2+} \propto Ap/(Bp+C)$ where A, B, and C are constants, as with I_+; but $I_{2+} \propto p^{\frac{1}{2}}$ from 5×10^{-7} to 10^{-8} torr, although $I_{2+} \propto p$ has been achieved in two cases. $I_{2+} \propto I_e^2$ under certain conditions of pressure and repeller potential, but under unfavourable conditions the variation may be far more rapid (figure 10). The variation of I_+ with repeller potential V_R shows narrow and broad regions (figure 5) which

might plausibly be attributed respectively to trap and free area processes; but $I_{2+}(V_R)$ (figure 6) shows the sharp peaking corresponding to trap area processes, and discussed in § 1 (*b*) above.

The processes that can lead to extraction or storage of positive ions include:

1. Leakage of ions from the circumference of the trap by the thermal process considered in § 1 (*c*). This will occur at a rate proportional to the ion density, which is denoted as $\kappa_1 n_+$ for singly charged ions, $\kappa_2 n_{2+}$ for doubly charged.

2. Extraction of ions by collisions with gas atoms. An ion oscillating radially and reaching almost the trap boundary may receive a marginal impulse from a thermal gas atom, sufficient to cause it to cross the boundary. This effect we believe to be unimportant. Assuming that a fraction F_1 of singly charged ion elastic collisions with gas lead to extraction, the rate is $F_1 \sigma_{\text{el.}} \bar{v}_{01} n_+ n_0$; the appropriate mean velocity $\bar{v}_{01}$ is thermal, and the elastic cross section $\sigma_{\text{el.}}$. However, gas collisions will also contribute to storage, in the following way:

3. Ions may in the course of their radial oscillations exchange momentum with gas atoms, some of them losing their power to reach the trap boundary, and thereafter spending their time in the trap centre from which extraction is more difficult. This 'gas collision storage', is believed to exceed the previous effect by quite a large factor, but still to be unimportant.

Moreover, ions formed outside the trap area can during their passage through it exchange momentum with gas atoms and be trapped. Assuming that a fraction G_1 of singly charged ion elastic collisions with a gas lead to storage, then the rate is $G_1 \sigma_{\text{el.}} \bar{v}_+ n_+ n_0$, with mean velocity $\bar{v}_+$ large compared to thermal.

4. Momentum exchange collisions with electrons can lead to longitudinal extraction of marginally trapped ions. This is unlikely to be an efficient process, on account of the intensity of the longitudinal trapping field and the small mass of the electron. For a fraction H_1 of effective collisions the extraction rate is $H_1 \sigma_e n_e n_+ v_e$, where σ_e represents the elastic electron-ion collision cross section.

5. Momentum exchange collisions between two positive ions can lead to the extraction of one of them; provided that the other starts from outside the trap area, and, having momentum to spare, can still remain untrapped after the collision. A number of such collisions will actually lead to storage, but on balance, some ion collision extraction will occur at all except the smallest ratio of free to trap area. For completely efficient trapping (zero free area), no such extraction process is expected. If a fraction J_1 of collisions can lead to extraction, and if σ_{++} represents the elastic collision cross section between two singly charged ions, then the rate is $J n_+^2 \bar{v}_+ \sigma_{++}$.

Ions can also be lost from the trap by inelastic collision processes; of these the most important are ionization by electrons, ion-atom clustering, and charge transfer.

6. The ionization rate of positive ions by electrons is $\sigma_{2i} n_e v_e n_+$, but the ionization rate of doubly charged ions is zero, since the experiments are conducted below the appropriate onset energy; so also is the rate of production of doubly charged ions from the gas by a single process. Radiative and dielectronic recombination between positive ions and electrons are neglected, since most of the electrons are non-thermal, and autoionization levels are rare.

PHILOSOPHICAL TRANSACTIONS OF THE ROYAL SOCIETY A MATHEMATICAL, PHYSICAL & ENGINEERING SCIENCES

7. Two-body clustering collisions of positive ions in their own gas lead to the depopulation of atomic ions

$$X^+ + X \rightarrow X_2^+ * \rightarrow X_2^+ ; \tag{32}$$

the excited molecular ion complex may be stablized radiatively or in collision with a third body. However, symmetrical resonance charge transfer

$$X^+ + X \rightarrow X + X^+ \tag{33}$$

has no depopulating effect, although it can contribute to thermalization of the ions.

If we confine the discussion to a single atomic gas, ion-atom interchange need not be considered. Process 32 is assigned a rate constant k_1. For molecular ions and gases ion-atom interchange processes contribute to this rate constant.

For doubly charged ions the single electron capture process

$$X^{2+} + X \rightarrow X^+ + X^+ \tag{34}$$

is always exothermic and must be taken into account. We assign it a rate constant k_2. Radiative charge transfer, and, for molecular ions and gases, ion-atom interchange processes, may contribute to this rate constant.

Heavy particle collisions leading to the formation of ions from other charge states (e.g. singly charged from doubly charged) will be neglected as storage processes, although they are considered as population loss processes.

For singly and doubly charged ions the complete kinetic equations are written

$$\underset{\text{process:}}{n_e v_e \sigma_i n_0} = \underset{1}{\kappa_1 n_+} + \underset{2}{F_1 \sigma_{\text{el.}} \bar{v}_{01} n_+ n_0} - \underset{3}{G_1 \sigma_{\text{el.}} \bar{v}_+ n_+ n_0} + \underset{4}{H_1 \sigma_{e1} n_e n_+ v_e} + \underset{5}{J_1 n_+^2 \bar{v}_+ \sigma_{++}} + \underset{6}{\sigma_{2i} n_e v_e n_+} + \underset{7}{k_1 n_+ n_0}; \tag{35}$$

$$\underset{\text{process:}}{n_e v_e \sigma_{2i} n_+} = \underset{1}{\kappa_2 n_{2+}} + \underset{2}{F_2 \sigma_{2\text{el.}} \bar{v}_{02} n_{2+} n_0} - \underset{3}{G_2 \sigma_{2\text{el.}} \bar{v}_{2+} n_{2+} n_0} + \underset{4}{H_2 \sigma_{e2} n_e n_{2+} v_e} + \underset{5}{J_2 n_{2+} n_+ \bar{v}_{2+} \sigma_{2+}} + \underset{6}{0} + \underset{7}{k_2 n_{2+} n_0}. \tag{36}$$

The production of currents I_+, I_{2+} of ions in the mass spectrometer is given by the following equations:

$$I_+ = \underset{\text{process:}}{\mathscr{E} A_T l \{} \underset{1}{n_+ \kappa_1} + \underset{2}{F_1 n_+ n_0 \bar{v}_{01} \sigma_{\text{el.}}} + \underset{3}{0} + \underset{4}{H_1 \sigma_{e1} n_e n_+ v_e} + \underset{5}{J_1 n_+^2 \bar{v}_+ \sigma_{++}} \} + \mathscr{E} A_F l n_+ / t_f; \tag{37}$$

$$I_{2+} = \underset{\text{process:}}{\mathscr{E} A_T l \{} \underset{1}{n_{2+} \kappa_2} + \underset{2}{F_2 n_{2+} n_0 \bar{v}_{02} \sigma_{2\text{el.}}} + \underset{3}{0} + \underset{4}{H_2 \sigma_{e2} n_e n_{2+} v_e} + \underset{5}{J_1 n_+ n_{2+} \bar{v}_+ \sigma_{2++}} \}. \tag{38}$$

We now proceed by trial and error to neglect certain terms in equations (35) to (38) with the object of obtaining solutions corresponding to the simple variations of ion current with pressure $p\,(\text{torr}) = 760 n_0 / 2{\cdot}7 \times 10^{19}$ and electron current observed in experiment. For example, if we wish to test the behaviour of the ion currents when electron collision extraction (process 4) is dominating, we neglect all terms except 4, arriving with the use of equation (15) and the assumption that $A_T = \mathscr{A}$ at

$$I_+ = \mathscr{E} \sigma_i n_0 I_e \mathscr{C} l, \tag{39}$$

$$I_{2+} = \frac{\mathscr{E} \sigma_{2i} \sigma_i n_0 I_e \mathscr{C} l}{H_1 \sigma_{e1}}. \tag{40}$$

This linear dependence of doubly charged ion current on pressure and on electron current is not in conformity with the experimental data. We therefore conclude that electron collision extraction (process 4) is not the dominant process; furthermore, its inclusion even as a correction destroys the correspondence of theory and experiment.

The most successful assumption is that the kinetics are dominated (at all except the lowest pressures) by thermal leakage and by heavy particle collisions. Neglecting processes 2, 3, 4, 5, 6 and 8, and for convenience taking $A_T = \mathscr{A}$, we have

$$I_+ = \mathscr{E} I_e l \sigma_i n_0 \kappa_1 \mathscr{C} / (\kappa_1 + n_0 k_1), \tag{41}$$

$$I_{2+} = \frac{\mathscr{E} I_e^2 \mathscr{C}^2 l}{A_T} \frac{\sigma_{2i} \sigma_i n_0 \kappa_2 \kappa_1}{(\kappa_1 + k_1 n_0)(\kappa_2 + k_2 n_0)}. \tag{42}$$

Here electron current dependence (assuming that $\kappa_2 \not\propto I_e$), and the pressure dependence (neglecting the term $k_1 k_2 n_0^2$) of I_+ and I_{2+} are as found in experiment. We find that $k_1 n_0 \ll \kappa_1$ for krypton; otherwise $k_1 n_0$ is undetectably small. The doubly charged ion pressure dependence is effectively $Ap/(Bp+C)$ where A, B and C are constants, but some additional features are found in the experimental data.

Since terms 2 and 3 in equations (35), (36) add up to a negative composite term, their inclusion as dominant terms would lead to a doubly charged ion current decreasing with increasing pressure. The inclusion of term 6, which is not demonstrably negligible until the values of κ_1 and k_1 are known, would lead to doubly charged ion dependence on current of the type $I_e^2/(A+BI_e)$. Neither of these is realistic.

Neglect in equations (39) to (42) of the contribution to I_+ from free area processes is not intended except as a convenience; equation (29) must be used whenever it is intended to take them into account; however, the neglect in equation (42) of the contribution to I_{2+} from free area processes is probably justified.

Equation (42) reduces to (29) when inelastic heavy particle collision processes are neglected. The effect of these processes is one of reducing the trapping time from its 'natural' value when only thermal leakage extracts the ions, to a shorter value, which is pressure dependent. Calculation of absolute values of k_1 and k_2 from the data is possible (see § 4 (*c*)) only if the assumption is made that $\kappa_1 = \kappa_2$, and if equations (18) to (22) are relied upon. But relative magnitudes might easily be inferred from experiments with mixtures.

No estimates of the magnitudes of the terms 2 and 3, $(F_1 - G_1)\,\sigma_{\mathrm{el.}}$, can be made from the data except that they are negligible.

The pressure dependence of I_{2+} shows a marked departure from the form $Ap/(Bp+C)$ in the lower pressure range (figure 8 *b*), and except in the cases of argon and xenon does not show the linear pressure dependence which equation (42) would imply in the low pressure limit. Instead, $I_{2+} \propto n_0^{\frac{1}{2}}$ (figure 8 (*a*)). One must therefore conclude that another collisional extraction process becomes dominant at low pressures; the obvious candidate is the ion-ion collision mechanism (5) already considered. At lower pressures the ions are less quickly thermalized by momentum exchange with gas molecules, and their loss by inelastic conversions during trapping time is also smaller. The fast ion-ion collisions taking place in the free area become more important. Neglecting terms 1, 2, 3, 4, 6, 7 and 8 in equations (35) to (38) and again assuming $A_T = \mathscr{A}$, one arrives at equation (39) and also

$$I_{2+} = \mathscr{E} l A_T^{-\frac{3}{2}} \sigma_{2i} I_e^{\frac{3}{2}} \mathscr{C}^{\frac{3}{2}} \sigma_i^{\frac{1}{2}} n_0^{\frac{1}{2}} (J_1 \sigma_{++} \bar{v}_{++})^{-\frac{1}{2}} \tag{43}$$

which exhibits the pressure dependence observed experimentally. Since I_{2+} is much smaller at the lower pressures, a check on the $I_e^{\frac{3}{2}}$ dependence has not yet proved possible. It is of interest to note that the inclusion of term 6, which cannot be shown to be negligible in this case, unless the values of J_1, J_2 are accurately known, leads to an equation in which I_+ has a polynomial variation with I_e:

$$I_+ = A + BI_e + CI_e^2. \tag{44}$$

Such a feature is not unknown (see figure 9, CO^+, Ne^+), so that ion collision extraction might be of importance at somewhat higher pressures than has been implied. However, variation of κ_1 with I_e is an alternative explanation.

For more intense electron currents ($I_e \sim 100\,\mu$A) than have been used in these experiments, the $I_+(I_e)$ function passes through a maximum and falls rapidly (figure 9, Kr^+). This can only be due to variation of κ_1 with I_e. As I_e is increased, the electron potential trap becomes deeper and κ_1 smaller, even though n_+ increases. $k_1 n_0$ can no longer be neglected in comparison with κ_1 (no more can $\sigma_{2i} n_e v_e$), so that we expect I_+ to fall off with increasing I_e. In general we seek to avoid this region of experiment, and obtain $I_+ \propto I_e$, $I_{2+} \propto I_e^2$ as closely as possible.

3. Experimental detail

Sections of our electron impact chamber (British A.E.I. mass spectrometer MS 10) are shown to scale in figure 1; minor modifications to the commercial instrument have been as follows:

(1) Substitution of a 0·5 mm wide oxide-coated ribbon for the rhenium filament, in order to minimize thermal dissociation of molecules and similar unwanted effects. Neither filament completely 'covers' the 1 mm diameter orifice through which the electrons pass. The 0·1 mm radii of curvature of 20 eV electrons in the 1830 G magnetic field will go some way towards rendering the beam cylindrical in the collision region, as we have considered it in § 1.

(2) One of the side plates has been removed from the chamber for reasons unconnected with the present experiments. No essential difference to the observations results from this feature; in fact a more uniform transverse electric field would result from removing both side plates.

(3) The electron collector has been held at 10 V positive to the impact chamber rather than the 35 V normally used in the instrument; the penetration of collector field is thus minimized to a point where interference with appearance potential functions is inappreciable.

(4) Resolving slits have been changed from those in the commercial form of the instrument: the electron impact chamber extraction slit is followed at a distance of 2 mm by a slit 12·0 × 0·25 mm which serves as the first resolving slit of the 180° system of 5 cm radius. The second resolving slit is 12·5 × 0·5 mm, and there is also a wide slit 12·6 × 3·7 mm at 90°. A resolving power of about 100 is achieved.

The ion collector is connected, with efficient electrical screening, to a Cary model 31 vibrating reed electrometer whose output feeds a Moseley model 135 XY pen recorder. Time constant effects are avoided by taking all pen records (except mass scans) first in one direction, then in the other. Since they superpose, only one direction is shown in figures 3, 4. Mechanically driven potential dividers are used for time-scanning of repeller-to-chamber potential V_R and electron impact chamber-to-filament potential V_e. But only a small

number of values of stabilized electron current I_e passing through the chamber have been available.

The instrument is connected in a bakeable vacuum system with ultimate pressure 5×10^{-10} torr, obtained by a separately bakeable Al_2O_3 trap above silicone oil diffusion pumps, there being also a Varian 15 l./s 'vacion' pump in the system. With gas inlet valves open to the glass cylinders the ultimate is still $\leqslant 10^{-9}$ torr.

In all experiments complete mass spectra are taken, and the residual gases found to be about equal proportions of carbon monoxide and hydrogen, with traces of methane and, with the 1 in. valve to the Al_2O_3 trap closed, helium. Total pressures are measured on a RG75P Bayard–Alpert type gauge with oxide cathode; its molybdenum grid is gold-plated (Petermann & Baker 1965). A supplementary molybdenum grid serves, when heated, to liberate pure carbon monoxide for the appropriate experiments. Noble gases are admitted through a $\frac{1}{4}$ in. Granville Phillips metal valve, and variation of the pumping rate as well as of the gas inlet rate is possible.

The gauge sensitivity is given by the manufacturers as 100 μA/mtorr at 10 mA grid current in N_2. The pressure measurements are made using this specification, and for other gases we use relative sensitivities given by the manufacturers as follows:

N_2 1·0; CO 1·04; He 0·16; Ne 0·25; Ar 1·22; Kr 1·86; Xe 2·7.

It is not considered that this procedure yields absolute pressures to better than $\pm 30\%$ or relative pressures to better than $\pm 20\%$.

In the measurements on methane the proportions of other gases present are very high, since the methane is obtained simply by switching off the vacion pump, which also yields other gases in accordance with its past history. Ionization gauge measurements are in this case rejected in favour of partial pressures obtained by applying the specifications of the mass spectrometer.

4. Analysis of data

The data are represented in figures 3 to 10 in the following forms: $I_+(V_e)$ (I_e) (p) (V_R) and $I_{2+}(V_e)$ (I_e) (p) (V_R). It is apparent that the principal features of the theory are justified by the measurements, but departures from ideal trap conditions are evident. When examining the effect of varying one parameter, extremely careful control of the invariance of the others is necessary.

(*a*) *Appearance potentials and peak shapes*

Mass number scansion peak shapes are not reproduced graphically, but the peak shapes show no unusual features, the I_{2+} being of similar shape to the I_+, except in the case of the mass number 10 Aston peak attributed to Ne_2^+ dissociation and discussed in § 4 (*f*) below. This current is of very diffuse scansion structure and can hardly be distinguished as a peak at all. Apart from this, the isotope abundances all check up satisfactorily.

The appearance potentials are deduced from figures 3 and 4, which are tracings of pen-recorder charts. It is difficult to determine appearance potentials with modern precision in this initial series of experiments, because the electron energy distribution is wide in this instrument, and with intense currents is seriously affected by the distribution of potential over the trapping region. Double differentiation of the He single ionization function yields an energy distribution shown in figure 3 (*a*) (inset). Certain trap processes (figure 4 (*a*))

display functions which indicate narrower distributions. In this situation it is not considered worthwhile to apply mathematical technique to the determination of the appearance potentials.

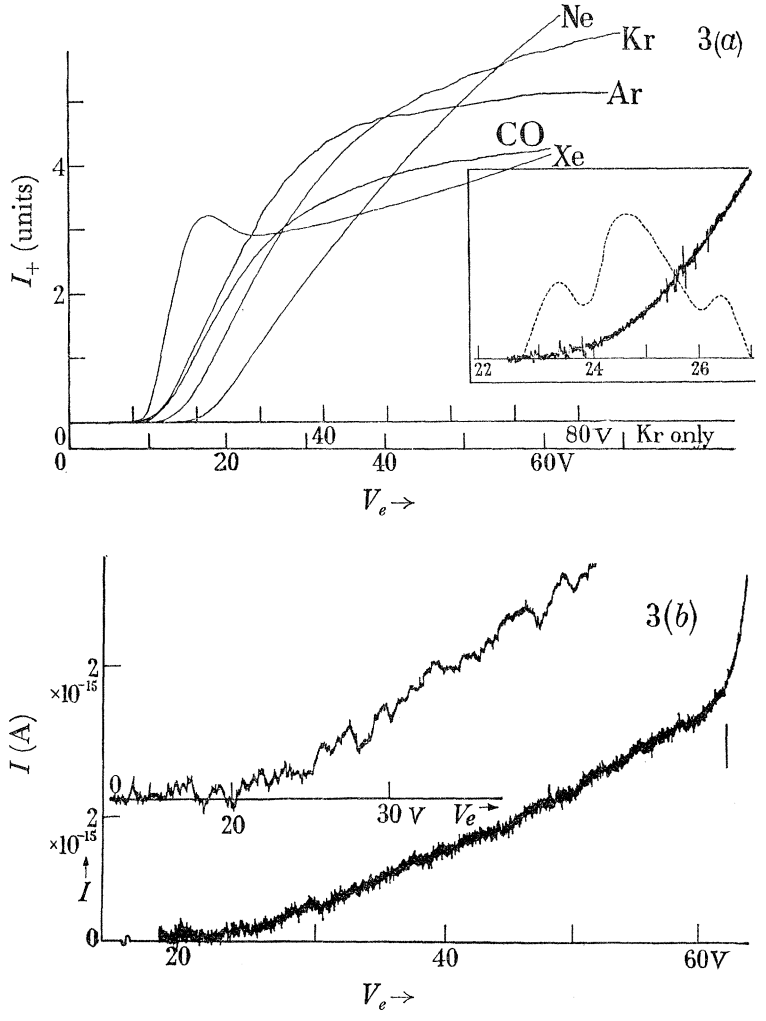

FIGURE 3. Functions I_+ (V_e) of singly charged ions and Aston peaks formed under the conditions:

		V_R (V)	I_e (μA)	p (torr)	units of current (A)
(*a*)	Ne^+	+1	48	$2{\cdot}8 \times 10^{-7}$	5×10^{-12}
	Ar^+	−1·5	48	$4{\cdot}3 \times 10^{-6}$	$1{\cdot}46 \times 10^{-10}$
	Kr^+	0	48	$3{\cdot}5 \times 10^{-7}$	10^{-12}
	Xe^+	+1	48	$4{\cdot}5 \times 10^{-7}$	5×10^{-13}
	CO^+	+1	48	$5{\cdot}2 \times 10^{-9}$	10^{-13}

Inset: onset of He^+ function, together with its second differential (dashed curve), obtained by computer program.

(*b*) Ne Aston peak mass 10 (below), $V_R + 3$ V, I_e 48 μA, p $2{\cdot}0 \times 10^{-6}$ torr; Ne mass 40 (above), $V_R + 1$ V, I_e 48 μA, p $8{\cdot}3 \times 10^{-7}$ torr.

It is found that the repeller potential V_R has a noticeable effect upon appearance potentials, and that the electron current has a small effect. Nevertheless, the appearance potentials for the rare gas processes shown in figures 3 and 4 present no real ambiguities, since the onset

energies (shown as vertical lines) are all well known and widely separated; we have adopted where possible the procedure of calibrating the electron energy scale against the appropriate ionization process involving only one electron impact. But it is found that the measured potential difference between impact chamber and filament, plus the potential V_R, does not depart from the single electron process calibration by more than 1 V.

The detection of ionization function 'breaks', even the widely separated ones (Hickam & Fox 1954) which should be seen in the CO^+ function of figure 3 (*a*), is difficult in the present experiments. Deconvolution techniques applied to Ar^{2+} (figure 4 (*b* 1)) yield structure at the lowest excited states of the ion.

However, the appearance potential and the piecewise linear structure of the ionization function threshold are of central importance to the identification of an electron impact process or sequence of processes. Therefore in further work it will be necessary to improve the accuracy of appearance potential measurement by any means possible. This is being done successfully in experiments in progress in a number of laboratories, with a view to exploiting fully the capabilities of this 'sequential' technique.

(*b*) *Repeller characteristics*

$I_{2+}(V_R)$ and $I_+(V_R)$ characteristics are shown in figures 5 and 6. The doubly charged ion characteristics show the sharp peaking at negative V_R, ($V_R(I_{2+})_{\max.} \propto m_+^{-1}$), and for Kr, Xe, there is a peak at positive V_R, as discussed in § 1 (*a*). The negative V_R peaks, being much easier to 'tune', have been used in all the data presented here.

FIGURE 4. Functions I_{2+} (V_e) of doubly charged ions and fragment ions formed under the conditions:

		V_R (V)	I_e (μA)	p (torr)
(*a*)	Ne^{2+}	−5	25·5	$1{\cdot}25 \times 10^{-6}$
			47·2	
			76	
(*b* 1)	Ar^{2+}	−3·5	47·5	$4{\cdot}5 \times 10^{-6}$
(*b* 2)	Ar^{2+}	−3·5	25·5	$4{\cdot}25 \times 10^{-6}$
			47·2	
			76	
(*c*)	Kr^{2+}	+1	47·5	$1{\cdot}86 \times 10^{-6}$
(*d*)	Xe^{2+} (1)	−0·5	9, 25·5, 48, 76	$4{\cdot}1 \times 10^{-7}$
	(2)	−1	9, 25·5, 48, 76	$9{\cdot}1 \times 10^{-7}$
(*e*)	CO^{2+}	+1	48	$5{\cdot}9 \times 10^{-7}$
(*f*)	C^+ from CO (1)	−5	76	$4{\cdot}25 \times 10^{-7}$
	(2)	−5	50	$6{\cdot}25 \times 10^{-6}$
	(3)	−5	9, 25·5, 48, 76	$4{\cdot}25 \times 10^{-7}$
(*g* 1)	CH_4^+, CH_2^+ from CH_4	−5	9, 25·5, 48, 76	$1{\cdot}7 \times 10^{-7}$
(*g* 2)	CH_4^+, CH^+ from CH_4	−5	9, 25·5, 48, 76	$2{\cdot}1 \times 10^{-7}$
(*h*)	Kr^{2+} in buffer trap	+1	25·5	(Ne) $9{\cdot}5 \times 10^{-7}$
			48	(Kr) $\sim 7 \times 10^{-9}$
			76	
(*j*)	Ne_2^{2+}	+1	48	$2{\cdot}5 \times 10^{-7}$
	Inset: mass scansion of peak 21·5 a.m.u.			
(*k*)	Xe^{3+}	−0·5	25·5	$3{\cdot}7 \times 10^{-7}$

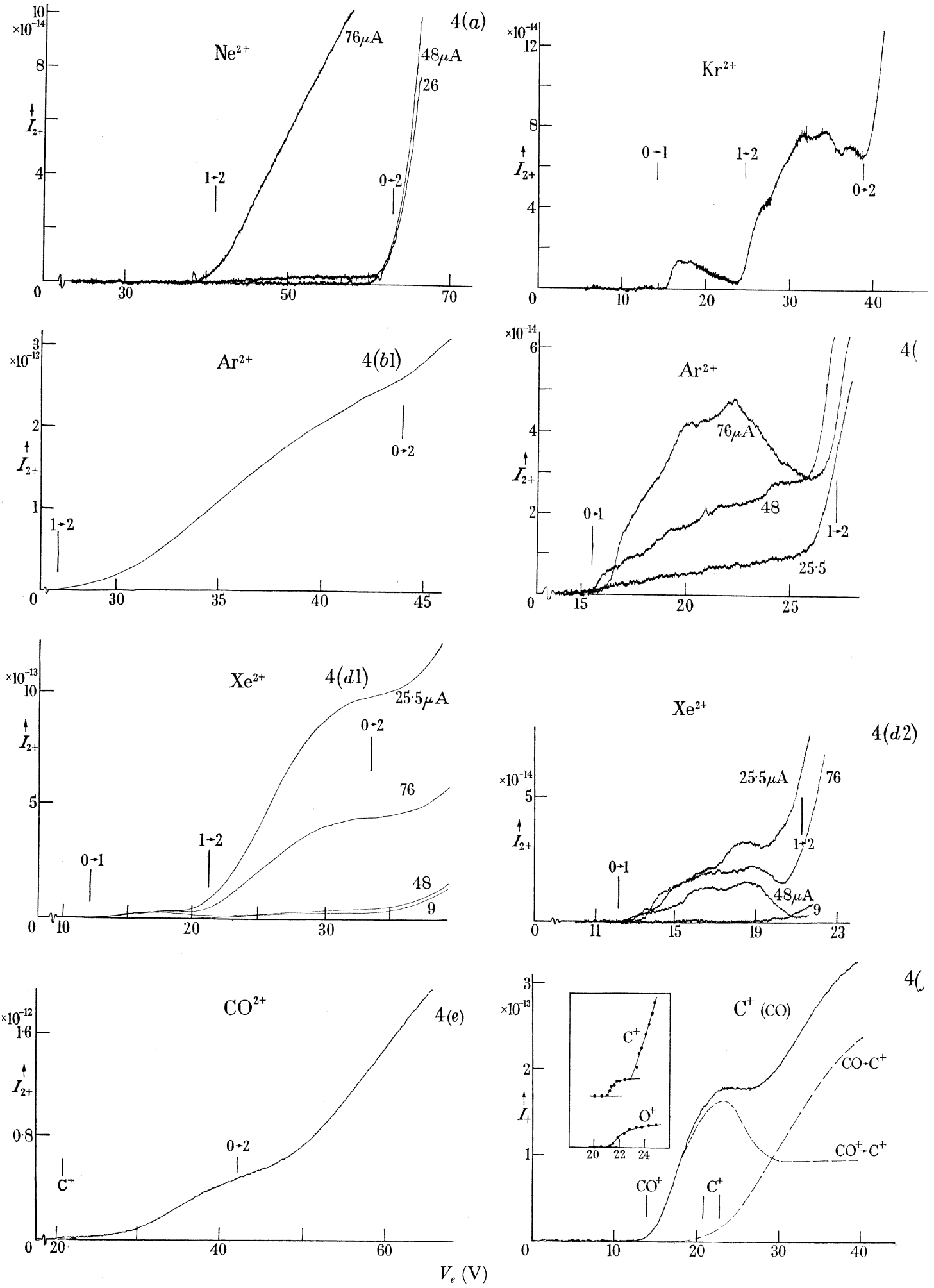

FIGURE 4. (For legend see p. 49.)

PHILOSOPHICAL TRANSACTIONS OF THE ROYAL SOCIETY A MATHEMATICAL, PHYSICAL & ENGINEERING SCIENCES

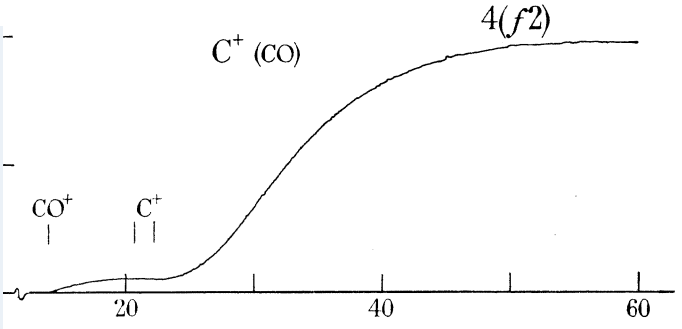

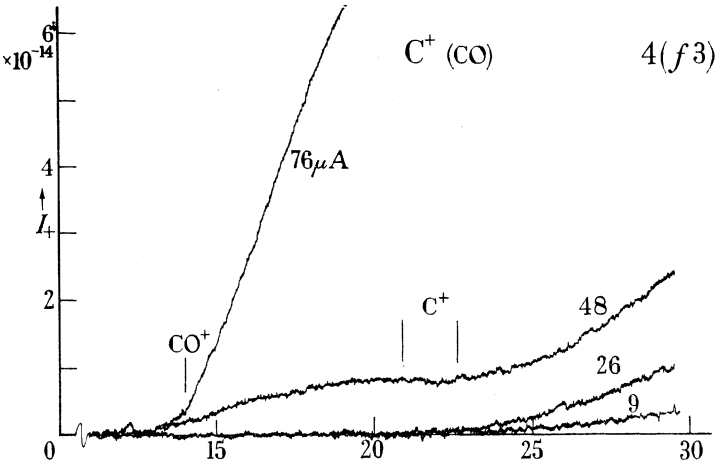

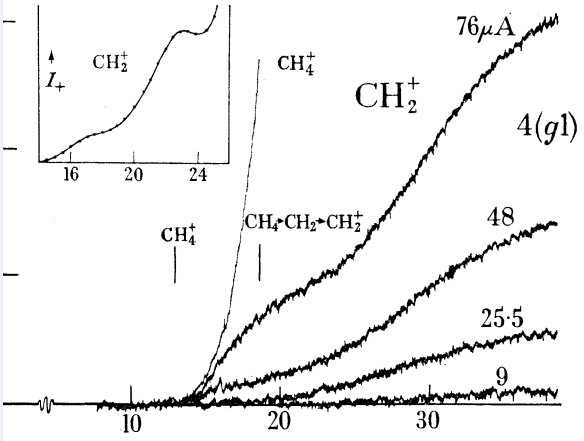

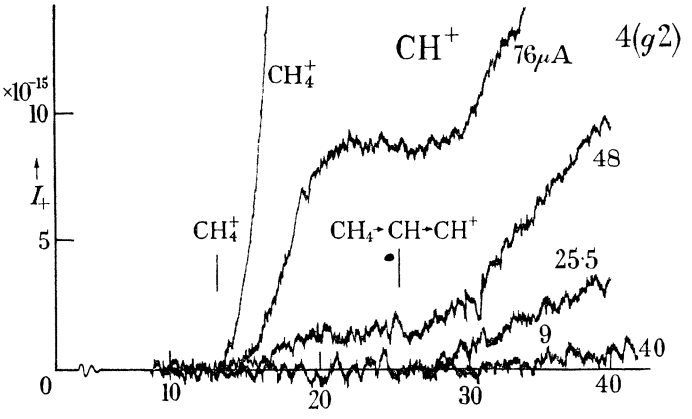

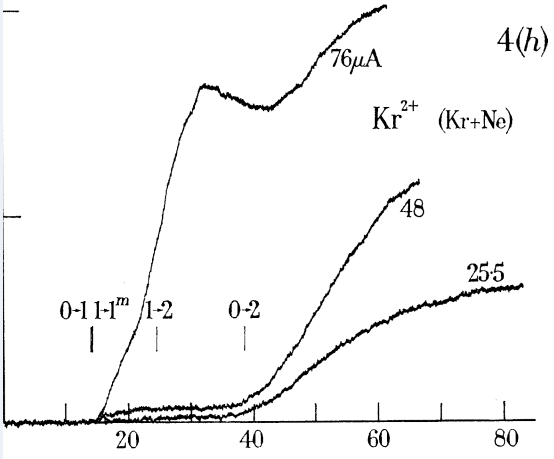

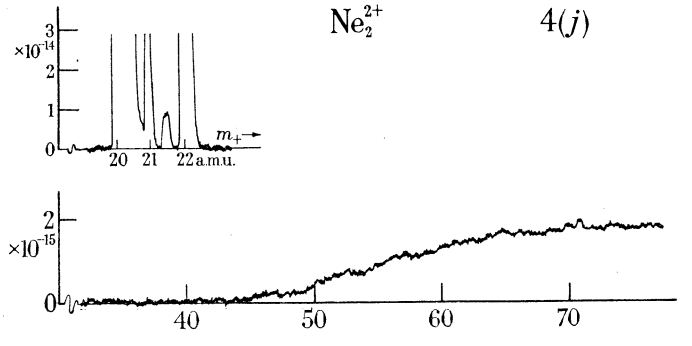

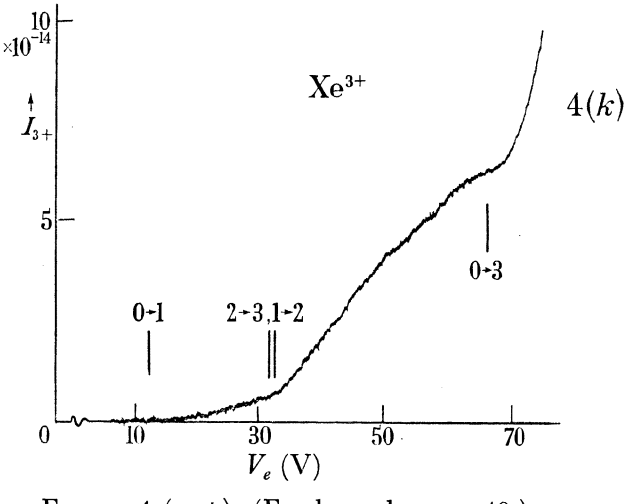

FIGURE 4 (*cont.*). (For legend see p. 49.)

The $I_{2+}(V_R)$ peak occurs closer to zero V_R for larger mass numbers, for which the field penetration is smaller.

A peaky structure is observed for the singly charged ion repeller characteristics $I_+(V_R)$. But it may be asked, why should I_+ increase with increasing trap area, since many positive ions are formed in the free area?

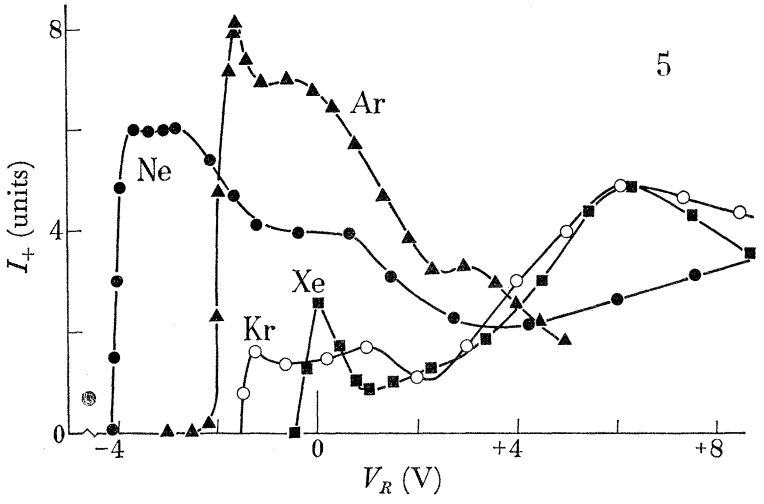

FIGURE 5. Repeller characteristics $I_+(V_R)$ of singly charged ions formed under the conditions:

		I_e (μA)	p (torr)	V_e (V)	units of current (A)
●	Ne^+	48	$1{\cdot}2\times10^{-8}$	70	10^{-12}
▲	Ar^+	48	3×10^{-6}	70	10^{-10}
○	Kr^+	48	$1{\cdot}8\times10^{-6}$	34	10^{-13}
■	Xe^+	48	$1{\cdot}0\times10^{-6}$	70	2×10^{-12}

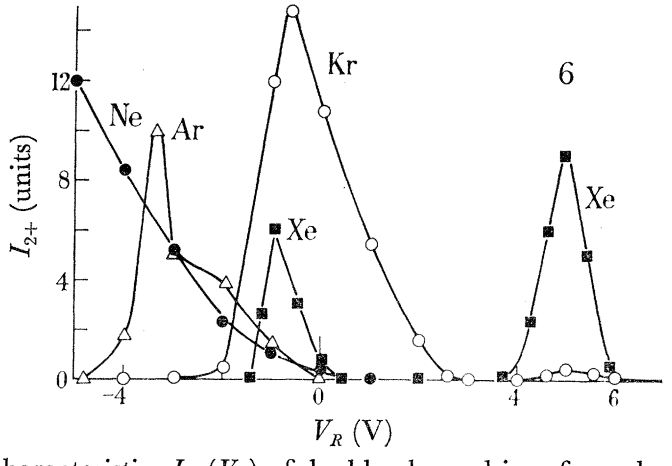

FIGURE 6. Repeller characteristics $I_{2+}(V_R)$ of doubly charged ions formed under the conditions:

		I_e (μA)	p (torr)	V_e (V)	units of current (A)
●	Ne^{2+}	76	1×10^{-6}	60	10^{-14}
▲	Ar^{2+}	48	$3{\cdot}8\times10^{-6}$	40	5×10^{-13}
○	Kr^{2+}	48	$1{\cdot}3\times10^{-6}$	34	10^{-13}
■	Xe^{2+}	48	1×10^{-6}	28	10^{-14}

The smooth positive V_R portions of the characteristics are for the most part attributable to free area, since extraction efficiency often increases with increasing V_R. However, longitudinal trapping influences I_+ extraction. Longitudinal trapping is only possible where there is also radial trapping, and within the trap area the singly charged ions congregate in the volume

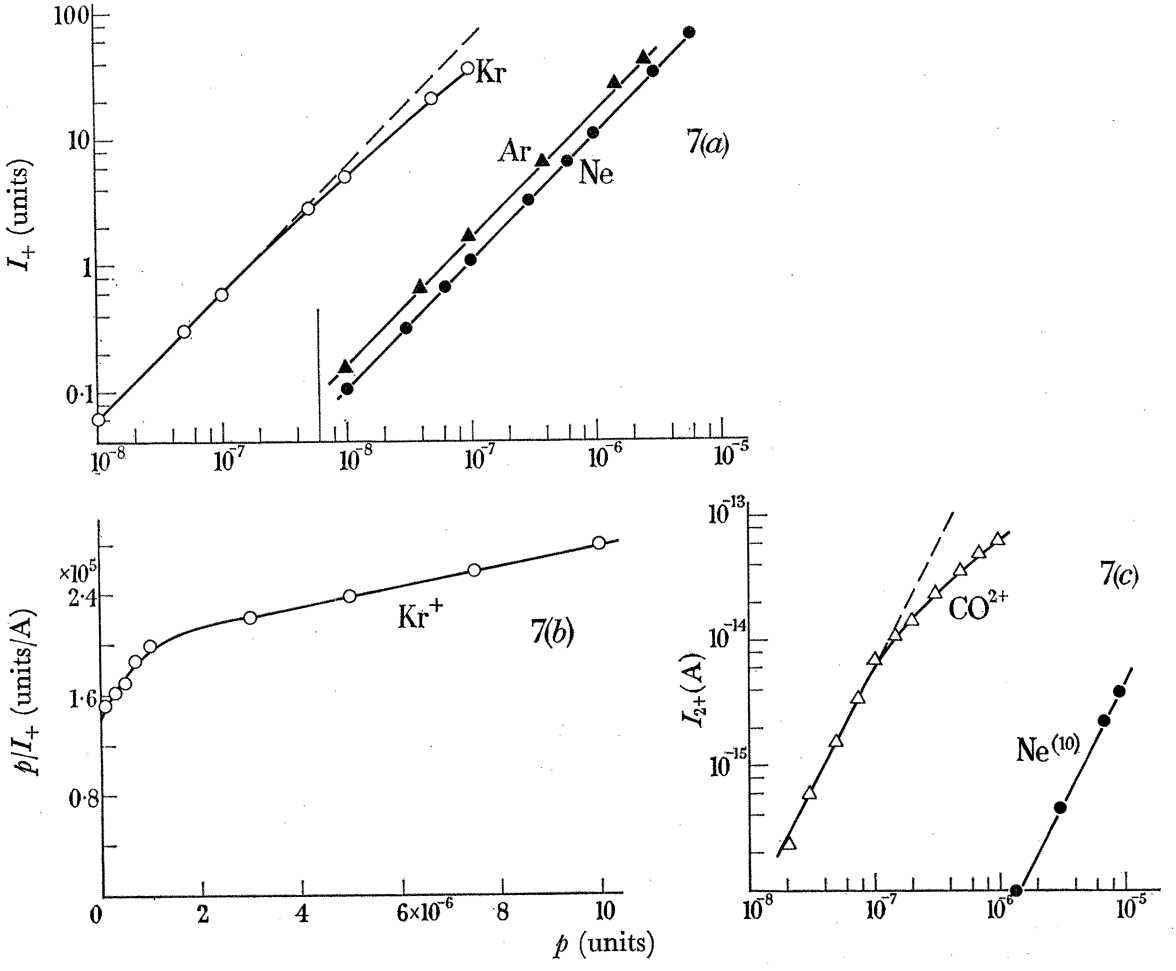

FIGURE 7. Pressure dependence (a, b) of singly charged ions, $I_+(p)$, and (c) Aston peaks etc., under the conditions:

(a, b)		V_R (V)	I_e (μA)	V_e (V)	units of current (A)	gauge units (torr)
●	Ne^+	+1	48	70	10^{-11}	0·25
▲	Ar^+	−1·5	48·5	45	10^{-11}	1·22
○	Kr^+	+1	47·5	34	10^{-12}	1·86
		Representations (a, c) logarithmic, (b) $p/I_+(p)$.				
(c)						
●	Ne mass 10	+1	76	65	—	0·25
△	CO mass 14	+1	48	40	—	1·04

directly above the extraction slit. In the free area such congregation is not possible, so that fewer ions are extracted (the factor $\mathscr{E}$ includes effects such as this). Thus the $I_+(V_R)$ characteristics show the general features of trap area dependance on V_R, in addition to the free area component. The double ionization process seems to detract from the $I_+(V_R)$ trap area peak most efficiently in Ar.

Mass scansion tuning depends upon the repeller potential in the manner expected, so that in taking repeller characteristics retuning is required for each value of V_R. Careful adjustment of V_R is required in all measurements of I_{2+} functions.

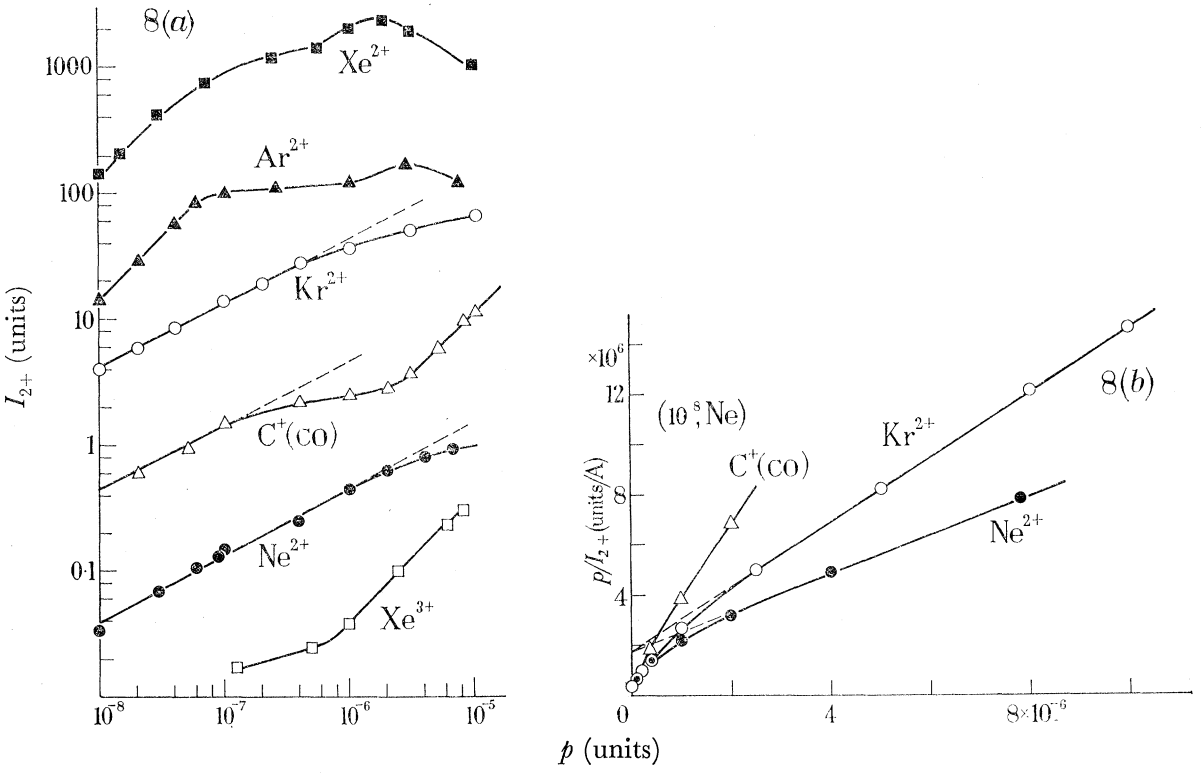

FIGURE 8. Pressure dependence of doubly charged ions, I_{2+} (p), under the conditions:

		V_R (V)	I_e (μA)	V_e (V)	units of current (A)	gauge units (torr)
●	Ne^{2+}	−5	76	60	10^{-14}	0·25
▲	Ar^{2+}	−3·5	48·5	45	10^{-15}	1·22
○	Kr^{2+}	+1	47·5	34	10^{-14}	1·86
△	C^+ from CO	−5	76	30	10^{-13}	1·04
■	Xe^{2+}	−1	25·5	30	10^{-16}	2·7
□	Xe^{3+}	−1	25·5	65	10^{-12}	2·7

Representation (*a*) logarithmic (*b*) $p/I_+(p)$.

(*c*) *Pressure dependence of ion currents*

Pressure characteristics of ion currents appear in figures 7 and 8, and have been discussed in § 2 (*b*), particularly equations (41), (42).

From figure 8 we see that the Ne^{2+}, Kr^{2+} and C^+ pressure functions are essentially similar (the sudden high pressure rise in the C^+ function is almost certainly attributable to C^+ from residual CH_4 ion-molecule reactions, and may be overlooked). At higher pressures the dependence is $Ap/(Bp+C)$ and at lower pressures $p^{\frac{1}{2}}$. The Xe^{2+} and Ar^{2+} functions are linear in p at lower pressures, and also saturate at higher pressures, although one would hesitate to fit them to $Ap/(Bp+C)$ exactly. The Xe^{3+} function is unique, and since a triple sequence of processes is involved (see section (*e*)), it will not be discussed further.

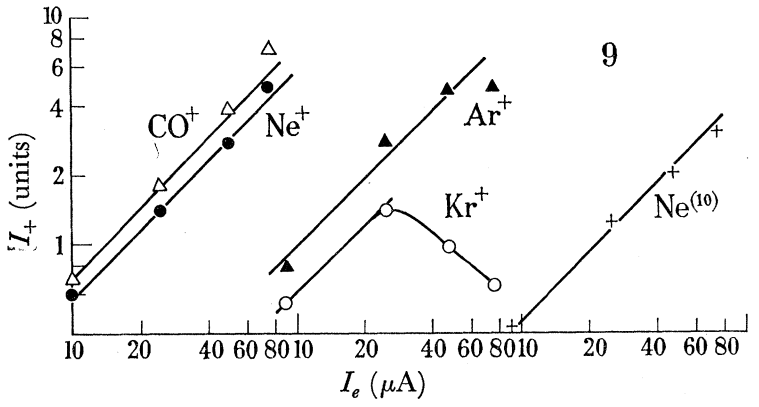

FIGURE 9. Electron current dependence of singly charged ions and Aston peaks under the conditions:

		V_R (V)	V_e (V)	p (torr)	units of current (A)
●	Ne^+	+1	30	$1{\cdot}2 \times 10^{-6}$	10^{-11}
▲	Ar^+	−1·5	40	$4{\cdot}2 \times 10^{-6}$	10^{-10}
○	Kr^+	+1	70	$2{\cdot}6 \times 10^{-7}$	10^{-13}
△	CO^+	+1	70	$5{\cdot}2 \times 10^{-9}$	10^{-13}
×	Ne mass 10	+1	35	$1{\cdot}75 \times 10^{-6}$	10^{-16}

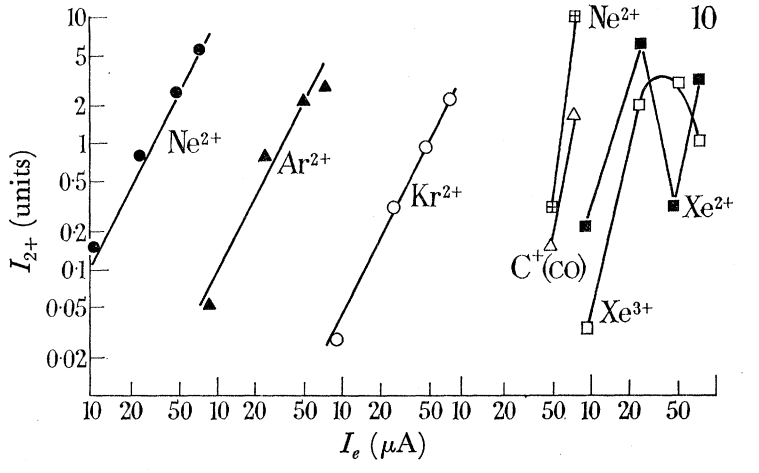

FIGURE 10. Electron current dependence of doubly charged ions $I_{2+}(I_e)$ and fragment ions under conditions:

		V_R (V)	V_e (V)	p (torr)	units of current (A)
●	Ne^{2+}	+1	55	$1{\cdot}7 \times 10^{-6}$	10^{-16}
⊞	Ne^{2+}	−5	65	$1{\cdot}25 \times 10^{-6}$	10^{-14}
▲	Ar^{2+}	−3·5	45	$4{\cdot}25 \times 10^{-6}$	10^{-12}
○	Kr^{2+}	−2	35	$2{\cdot}6 \times 10^{-6}$	10^{-12}
■	Xe^{2+}	−0·5	30	4×10^{-7}	10^{-13}
□	Xe^{3+}	−0·5	50	4×10^{-7}	10^{-13}
△	C^+ (CO)	−5	27	$4{\cdot}25 \times 10^{-7}$	10^{-14}

For the analysis of a dependence $I \propto Ap/(Bp+C)$ it is necessary to plot a graph of p/I against p, as in figures 7 (b), 8 (b); the slope gives B/A and the zero ordinate intercept C/A, so that the ratio of slope to intercept is equal to k_1/κ_1 for $I_+(p)$, and approximately

$$(k_1\kappa_2+k_2\kappa_1)/\kappa_1\kappa_2$$

for $I_{2+}(p)$. To obtain absolute values of k_1, k_2, it would be necessary to calculate κ_1 from equations (18) to (22), or alternatively take A_T/A_F arbitrarily equal to unity, which we now do. It is assumed that $\kappa_1 = \kappa_2$, so that both k_1 and k_2 may be calculated. For Kr, $\epsilon_T = 0{\cdot}021$ (see § 4 (e)) and using equation (31) and estimating t_f, we obtain

$$k_1 \sim 7\times10^{-15}\,\mathrm{cm^3/s}, \quad k_2 \sim 2\times10^{-13}\,\mathrm{cm^3/s}.$$

k_1 is appropriate to process 32 and k_2 to process 34. For Ne and Ar k_1 is too small to show any effect; we hesitate to calculate values of k_2 at this stage. But from data obtained in a gas mixture, ratios of k_2 values could readily be obtained.

In figure 7 the low pressure $I_{2+}(p)$ functions are represented logarithmically in order to display the one-half power dependence accounted for in equation (43). Using the assumed values of σ_{2i}, σ_i we can calculate the product $J_1\sigma_{++}\bar{v}_{++}$ from equations (39), (43). Taking $\bar{v}_{++}$ as the mean velocity corresponding to non-thermalized ions in a trap of depth 0·1 eV, and σ_{++} as a Coulomb cross section corresponding to this energy, J_1 for krypton ions is calculated to be *ca.* 0·001, which seems reasonable.

For argon and xenon the low pressure $I_{2+}(p)$ characteristics (figure 8) are linear, as is the case for a trap in which thermal leakage (term 1) is the only non-negligible process (equations (35) to (38)). These are the only experiments in which we have succeeded in achieving these conditions in a pure gas. They depend upon k_1 being small and V_R being correctly adjusted to give maximum I_{2+} (in Ne the available range of V_R did not permit this). At this value of V_R in argon, I_+ is extremely small, I_{2+} large, so that ϵ_T would be very high, probably close to unity. For measurements of Ar^+, however, it was considered better to off-tune V_R so as to obtain an easily detectable I_+.

(*d*) *Electron current dependence of ion currents*

The dependence of ion current upon electron current is shown in figures 9 and 10; the linear $I_+(I_e)$ and quadratic $I_{2+}(I_e^2)$ dependences are passably well maintained.

The value of $I_+(I_e)$ function measurements lies in their use for distinguishing between single electron and two electron processes. The Ar^{2+}, Kr^{2+} data adhere well to the square law, and justify the idea that κ_2 is largely independent of I_e in the working region. For the calculation of cross sections from the data, by means of equation (25), care is taken to choose data from a region where $I_+(I_e)$ is as closely linear as possible. For lighter atoms the extraction field penetration is greater, the trap weaker and accordingly the departure from quadratic $I_{2+}(I_e^2)$ more marked.

It would be premature to make detailed deductions about κ from the $I_+(I_e)$ functions, since no continuous variation of I_e is possible with the available electronics. However, the polynomial form of $I(Ne^+)$ (I_e) can be seen even from the four points on figure 9; the working region dominated by linear $I_+(I_e)$ is used for measurement.

The maxima in the $I_+(I_e)$ functions at large electron currents are probably associated with deep radial traps, in which many processes are preferred to the normal thermal leakage of

singly charged ions. These regions of intense I_e are avoided in the present experiments. The complicated $I_{2+}(I_e)$ function in xenon is probably attributable to inadequate tuning of V_R.

(e) *Calculation of cross sections*

From the data of figures 3 and 4, cross section functions are calculated from equation (25) for display in figure 11.

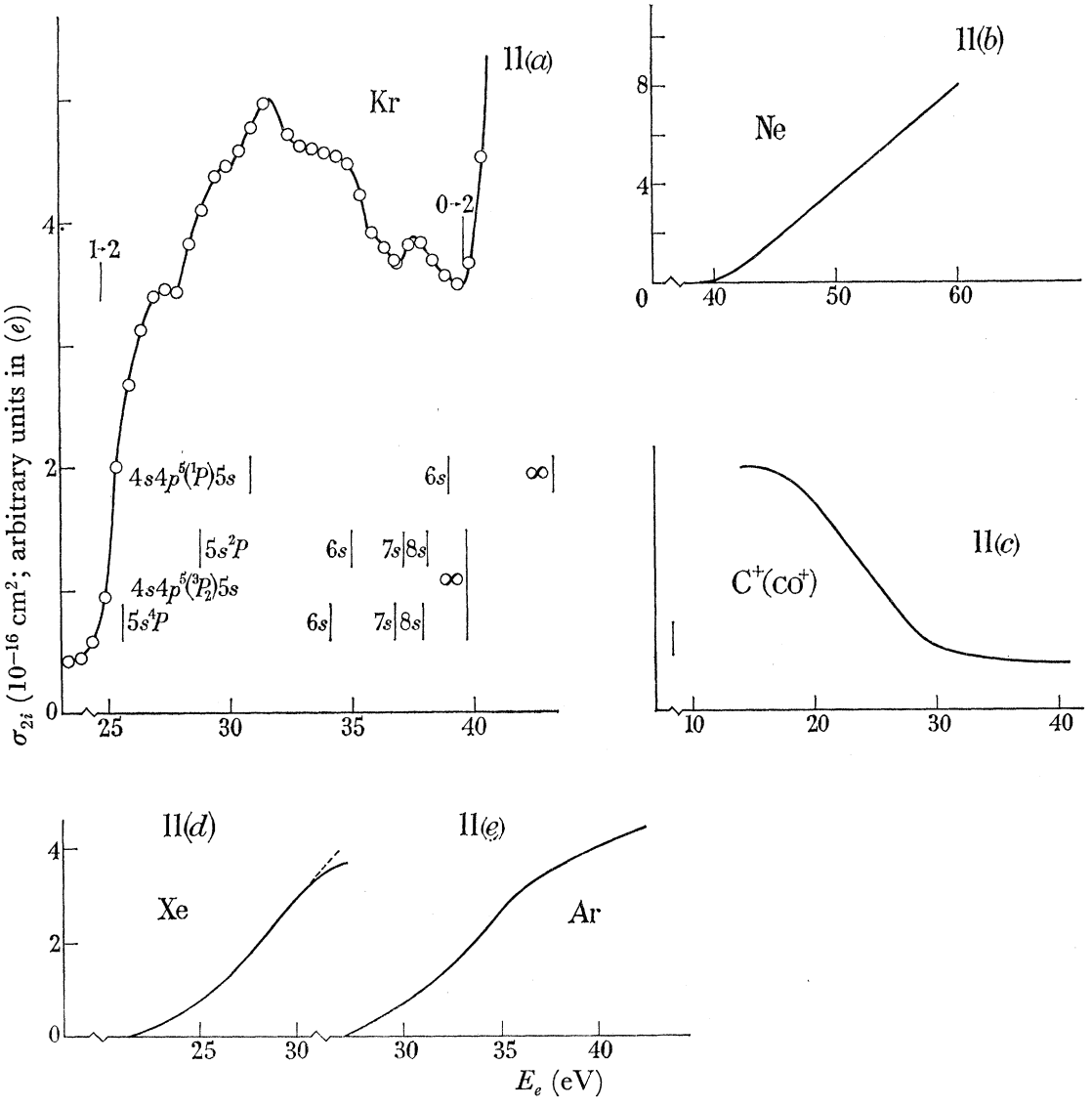

FIGURE 11. Cross section functions, calculated from equation (29) and data of figures 3 and 4 for ionization or fragmentation of positive ions, $\sigma_{2i}(V_e)$. (*a*) $Kr^+ \rightarrow Kr^{2+}$, (*b*) $Ne^+ \rightarrow Ne^{2+}$, (*c*) $CO^+ \rightarrow C^+$, (*d*) $Xe^+ \rightarrow Xe^{2+}$, (*e*) $Ar^+ \rightarrow Ar^{2+}$.

For normalization the values of σ_{2i} are chosen as follows:

gas	energy (eV)	ϵ_T	σ_{2i} (cm²)	source
Ne	60	0·00017	8×10^{-18}	Dolder *et al.* (1963)
Ar	40	0·002	*ca.* 5×10^{-17}	Kuprianov & Latypov (1963)
Kr	30	0·021	$2{\cdot}6 \times 10^{-16}$	Kuprianov & Latypov (1963)
Xe	30	0·23	$3{\cdot}1 \times 10^{-16}$	Kuprianov & Latypov (1963)

Also tabulated are the corresponding values of ϵ_T calculated from equation (29). It will be observed that there is a correlation between ϵ_T and the negative repeller potential necessary to balance the penetration of the extraction field.

For carbon monoxide no experimental value of σ_{2i} exists to which normalization can be made. A calculation based on the Coulomb–Born approximation is desirable, so that not only can σ_{2i} be normalized, but also the cross section for dissociation of CO^+, producing C^+, for which the identical ϵ_T might be used.

No account is given here of the work in progress on deconvolution of $I_+(V_e)$, $I_{2+}(V_e)$ functions, for artificially eliminating 'spread' arising from the distribution of electron energies in the experiment.

The voltage scale of the cross section functions follows directly from the voltage scale of the I_+, $I_{2+}(I_e)$ functions, which have been set where possible by the onsets of the single process.

(*f*) *Minimization of ion-molecule processes by the use of gas mixtures*

In the pressure region above 10^{-6} torr there is loss of both singly and doubly charged ions in the trap by inelastic heavy particle collisions. It is not always easy to minimize these losses by reducing the pressure, because once the lower pressure range ($\sim 10^{-7}$ torr) is reached, ion-ion collisions can cause extraction from the trap. Only in argon have we succeeded in avoiding this. Since only fast ions contribute to ion-ion collisional extraction, it becomes less important in the higher pressure range. But if a buffer gas is introduced, then the ions may be thermalized and ion-ion extraction minimized; moreover, the buffer gas may be chosen in such a way that the inelastic heavy particle collisions are inefficient, and that its own ionization is minimized.

Thus krypton may be investigated in the presence of a neon buffer, there being only small rate constants for the collision processes:

$$Kr^+ + Ne \rightarrow KrNe^{+*} \rightarrow KrNe^+, \tag{45}$$

$$Kr^+ + Ne \rightarrow Kr + Ne^+, \tag{46}$$

$$Kr^{2+} + Ne \rightarrow Kr^+ + Ne^+ + \Delta E, \tag{47}$$

$$Kr^{2+} + Ne \rightarrow Kr + Ne^{2+}. \tag{48}$$

Processes (46) and (48) are endothermic and strongly adiabatic. Process 47 is exothermic and may proceed via a pseudo-crossing of potential energy curves. But since the nuclear separation of this crossover

$$R_x \simeq 27{\cdot}2/\Delta E \quad \text{a.u.} \tag{49}$$

is *ca.* 9 a.u., one may estimate the rate to be 10^{-14} to 10^{-15} cm^3/s, following the method of Bates & Moiseiwitsch (1954) (see also Hasted, Lee & Hussain 1963).

The clustering process (45) is unlikely both in view of the large ionic radius of the krypton and the small polarizability of the neon, but we can assign no plausible rate to it.

If the ion-ion extraction and the inelastic losses are so minimized, it is possible to approach a trapping time limited only by thermal leakage. Results of a measurement of Kr^{2+} from a trap containing $3{\cdot}8 \times 10^{-6}$ torr Ne and 7×10^{-9} torr Kr are shown in figure 4 (*h*). The

krypton pressure is sufficiently low for the single process $e+\mathrm{Kr}\rightarrow\mathrm{Kr}^{2+}+2e$ to be reduced to the same order of magnitude as the double process at $I_e = 76\ \mu\mathrm{A}$. The cross section function is more or less normal, except for an enhancement of the triple process at the low-energy extreme.

By comparison of figure 4 (h) with (c), for which $\epsilon_T = 0{\cdot}021$, we calculate $\epsilon_T = 0{\cdot}13$ which are the most successful conditions we have achieved in krypton.

The requirements of a good buffer gas are understood to be: small interaction rates with reactant gas singly and doubly charged ions; single ionization cross section small compared with that of the reactant gas. Helium usually satisfies these requirements best, although its power of momentum exchange is small.

(g) *Measurements with molecular rare gas ions*

The deduction of the rate k_1 of the singly charged ion clustering process 32 has been discussed above in terms of the pressure dependence of I_+. For both argon and neon, the two-body process of the type

$$\mathrm{Ne}^+ + \mathrm{Ne} \rightarrow \mathrm{Ne}_2^{+*} \rightarrow \mathrm{Ne}_2^+ \tag{50}$$

possesses too small a rate to make an observable difference to the I_+ pressure function. However, the mass 40 ion is detectable in neon and the function $I_2(V_e)$ is shown in figure 3 (b). It is usually assumed that molecular rare gas ions are formed by the Hornbeck–Molnar process, involving metastable neutrals and ground state atoms

$$\mathrm{Ne}^m + \mathrm{Ne} \rightarrow \mathrm{Ne}_2^+ + e. \tag{51}$$

One might attempt to decide between processes (50) and (51) on the basis of appearance potential. The molecular ion current I_2 is proportional to p^2 (as in figure 7 (c) for the neon Aston peak), which is appropriate to either of the processes. Unfortunately the evidence of figure 3 (b) (energy scale calibrated against the single process for the formation of doubly charged ions from neutrals) is inadequate to decide between the appearance potential of a highly excited metastable neutral (Latypov, Kupriyanov & Tunitskii 1964) and that of the positive ion. Proceeding as before, we have equations (23) and (25) and also

$$I_2 = \mathscr{E} n_2 A_T l \kappa_2, \quad n_2 = n_+ n_0 k_1 / \kappa_2, \tag{52}$$

where κ_2 is the molecular ion extraction rate and n_2 its density. Assuming $A_T = A_F$,

$$\frac{I_2}{I_+} = n_0 k_1 t_f. \tag{53}$$

Equation (53) yields a rate $k_1 \sim 10^{-9}\,\mathrm{cm^3\,s^{-1}}$. It is much larger than those which show up as $Ap/(Bp+C)$ dependence in I_+ and I_{2+} data. It follows that ground state ions are not involved in the production of Ne^{2+}.

The ion Ar_2^+ (mass 80) could not be detected because of interference from an isotope of residual krypton. The $(\mathrm{CO})_2^+$ ion was searched for, but any current at mass number 56 was less than 10^{-16} A ($p = 10^{-6}$ torr, $V_e = 70$ V, all values of V_R) indicating that k_1 for CO is very small indeed.

PHILOSOPHICAL TRANSACTIONS OF THE ROYAL SOCIETY A MATHEMATICAL, PHYSICAL & ENGINEERING SCIENCES

As has been mentioned in § 2 (*a*) (7), the two-body clustering process for Kr^+ presumably proceeds via a long lived molecular ion excited state, which subsequently stabilizes radiatively or by collision with a third body.

5. Cross section functions and their interpretation

The cross section functions shown in figure 11 exhibit certain interesting features. Discussion of the peaked functions appearing at very low energies in figures 4 (*b* 2), 4 (*c*), 4 (*d* 2) will be deferred until after equation (55).

The ionization function for Ne^+ by electrons is closely linear with energy in this region and exhibits no detectable structure. The Ar^+ and Xe^+ functions exhibit curvature close to the upper energy limit, but no structure. It is possible that this curvature depends upon the conditions of the experiment and is instrumental in origin. Its elimination may in the future serve as a test of the quality of the trap and the efficacy of current scaling procedure (§ 1 (*a*)).

However, the ionization function for Kr^+ is dominated by structure which is presumably attributable to autoionization. The structure is repeatable under variation of pressure, electron current, and repeller potential, although there are certain conditions under which a wide distribution of electron energies can smooth out the details. Autoionization levels have been reported in Kr (Huffman *et al.* 1963) but not previously in Kr^+.

The V_e scale is normalized by means of the onset of the single process at 38·6 eV, and since it is unclear whether or not a linear increase should be observed above this energy (Fox 1960; Dorman & Morrison 1961), the extrapolation technique has not been used.

The onset for the electron-ion ionization process appears well up the observed ionization function, which may be significant from the point of view of autoionization. Quantum theory calculations of excitation of ions by electrons (Burgess 1961) yield cross section functions which are relatively large at threshold, above which a monotonic variation with energy is observed; in contrast with those for the excitation of neutral atoms, which are in general zero at threshold. The convolution of electron energy distribution with a nonzero onset cross section function

$$\bar{\sigma}(E) = \frac{\int \sigma(E) f(E)\, \mathrm{d}E}{\int f(E)\, \mathrm{d}E} \tag{54}$$

will resemble figure 11 (*a*) much more clearly than will the convolution with a zero onset cross section function. Pending the completion of a computer deconvolution program we arbitrarily place our onsets half way up an autoionization peak, in order to interpret the data in terms of an autoionization series. The first differential of the onset yields an electron energy distribution with wings as in figure 3 (*a*) (inset).

There are three likely possibilities of two excited electron series in Kr^+, a doublet and a quartet series of converging to $4s4p^5\,{}^3P_2$ and a doublet series converging to $4s4p^5\,{}^1P$ (ignoring fine structure). Both these limits are known. It is clear that any series possessing a term at 24·6 eV and converging to either of these limits would be unable to account for terms at 27·7 and 29·0 eV. These terms could therefore only be imagined to belong to the other two series. In such a situation it seems hardly worthwhile to attempt detailed Rydberg fitting. But a Ritz series

$$\sigma = -\frac{10\,9679}{(\Delta+n)^2} \tag{55}$$

giving the terms in wave-numbers for principal quantum number n and a constant defect Δ, will lead to the vertical lines shown in figure 11 (a).

Turning now to the low energy peaks which appear in figures 4 (b2), (c) and (d2); these have been neglected in calculating the Kr^+, Ar^+ and Xe^+ ionization functions. There are two possible interpretations, namely an Aston process in which the molecular ion dissociates in the mass-spectrometer, as is observed in neon; and a triple sequence of the type:

$$e + Kr \rightarrow Kr^+ + 2e, \tag{56}$$

$$e + Kr^+ \rightarrow Kr^{+m} + e \quad \text{(metastable ion)}, \tag{57}$$

$$e + Kr^{+m} \rightarrow Kr^{2+} + 2e. \tag{58}$$

There are two reasons for discarding the Aston process interpretation; first, the effect is not strongly pressure dependent and is enhanced when the krypton pressure is reduced to 5×10^{-9} torr in the buffered trap experiments; secondly, the $I_{2+}(I_e)$ dependence is higher power than quadratic (figure 10, open circles), supporting the view that a triple sequence is involved.

The $^4D_{\frac{7}{2}}$, $^4F_{\frac{9}{2}}$, $^4F_{\frac{7}{2}}$ and $^2F_{\frac{7}{2}}$ Kr^+ levels are metastable (Hagstrum 1956) and have energies $\geqslant 14{\cdot}9$ eV above Kr^+. Thus processes (56) to (58) are energetically possible at 14·9 eV, and must be considered likely candidates. Similar arguments apply to the argon and xenon data. The reasons for the loss of peak structure in the buffered krypton trap are not at all clear, but it may be that more complicated sequences contribute.

The complications in interpreting triple sequences make this an unprofitable field for detailed analysis, but the low energy peaks might with some plausibility be attributed to excitation functions.

Similar complications apply to the Xe^{3+} data of figure 4 (k). The onset at the ionization potential of Xe and the obvious 'break' at the appearance potential of Xe^{2+} suggest that the first of the sequential processes is that producing Xe^+ from Xe (or Xe^{2+} from Xe at the break). Many different possibilities arise in this sequence, and detailed analysis is unprofitable; the data is reproduced in order to draw attention to the possibilities of sequential production of multiply charged ions in hot plasmas.

We now consider the 'Aston peaks' which are responsible for certain of the data in Ne. It is well known (Hipple, Fox & Condon 1946; McGowan & Kerwin 1962) that an ion of (initial) mass number m_i, accelerated in a mass-spectrometer, converted into an ion of (final) mass number m_f and magnetically deflected, will be registered as an ion of apparent mass number m^*, where

$$m^* = m_f^2/m_i. \tag{59}$$

Thus the collisional dissociation of Ne_2^+ ions will produce ions of apparent mass number 10. These possess (figure 3 (b)) the same appearance potential as that of mass number 40 (figure 3 (a)), and may readily be distinguished from two electron sequence products by their pressure dependence, which is square law (figure 7 (c)), in contrast to $Ap/(Bp+C)$ (figure 8 (c)).

Further checks which have been made are that I_* is proportional to I_e, and that I_* (V_e) (figure 3 (b)) follows the form of $I_+(V_e)$.

It is important to eliminate Aston peaks carefully in studies of two electron sequences. This is achieved by control of the repeller potential to ensure maximum trap area, thus

maximizing the two electron sequences and leaving the Aston peaks unchanged (especially if Ne_2^+ is formed from a metastable neutral as in process (51)). Reduction of gas pressure and augmentation of electron current will have a similar effect.

We have not deduced any cross sections from Aston peak measurements, believing that the mechanism of dissociation of the molecular ion is not necessarily pressure-dependent (Daly 1965); it could be either a gas collision process, a natural decay, or a collision with a slit edge.

The mass scansion peak shape in neon is found to be so wide as barely to be distinguishable from the neighbouring and powerful mass 12 with the comparatively low resolution of our instrument. Thus the isotope abundance check has not proved possible.

We considered that the mass 14 current from CO (figure 4 (*e*)), being proportional to p^2 (figure 7 (*c*)), was likely to be an Aston peak; but our failure to observe $(CO)_2^+$ makes this impossible. The appearance potential and pressure dependence are such that the CO^{2+} ion could well be formed by the process

$$C^+ + O^+ \rightarrow CO^{2+} \qquad (60)$$

in which one of the atomic ions (not necessarily C^+) carries internal excitation to make up the necessary energy difference. The form of the potential energy curves is such that tunnelling is possible, and we submit that such processes must be considered as candidates for formation of molecular double charged ions. No accurate estimation of the internal excitation of either ion can be made from study of the CO^{2+} appearance potential, nor is it established that the CO^{2+} is formed in the ground state in this collision.

An interesting observation has been made of a Ne_2^+ isotope peak at mass number 21·5 (the 20·5 peak, which should also appear, is lost in the powerful mass 20). The peak resolution is shown in figure 4 (*j*), together with the $I(V_e)$ function, which shows an onset at 45 ± 5 eV. This peak can only be interpreted as Ne_2^{2+} (isotopes 21 and 22), presumably formed by the ionization of Ne_2^+ by electrons. No estimate of the magnitude of the cross section for this process has been possible, but the form of the function is of interest.

The dissociation of the carbon monoxide ion CO^+ by electrons can be studied using the ion trap technique. Unfortunately the production of the important O^+ ion cannot yet be investigated, because of interference from mass 16 CH_4^+, which is always present at small partial pressures in this apparatus. However, the interference of methane with the mass 12 C^+ is easily shown to be unimportant. The $I(C^+)V_e$ functions are displayed in figure 4 (*f* 1, 2, 3) and using the $I(CO^+)V_e$ data of figure 3 (*a*) we calculate a cross section function as in figure 11 (*c*).

This function presumably possesses a maximum below 14 eV. The fast rate of falloff is important because of the assessment of the exact importance of ion dissociation by electrons in fragment ion mass-spectrometry, conducted typically at $V_e = 70$ eV. The entire C^+ function up to this energy is shown in figure 4 (*f*).

In calculating figure 11 (*c*) we have assumed that there is no contribution in the region $V_e = 20{\cdot}0$ to $22{\cdot}8$ from the process producing C^+ and O^- (Hagstrum 1951). The best calibration of our energy scale appears to be from the double process, which becomes possible at 14 eV. On this basis the rise of C^+ current at higher energies extrapolates to an appearance potential very approximately 23 eV.

Thus the process with onset at 20·9 eV, which appears in Hagstrum's figure 10 (data reproduced as inset to figure 4 (f)), is not seen clearly to contribute to the C^+ function; it may nevertheless be present, but obscured because too small.

The reality of the 20·9 C^+ appearance potential is supported by the appearance of O^- at the identical energy, and by the fact that the energy balance is correct

$$\left.\begin{aligned} &E_i(\mathrm{C})+D(\mathrm{CO})-E_a(\mathrm{O}) = 20{\cdot}92\,\mathrm{eV},\\ &11{\cdot}26+11{\cdot}11-1{\cdot}45. \end{aligned}\right\} \tag{61}$$

But a plausible case could be made for O^- production by dissociative recombination of $CO^+ B^2\Sigma_u^+$, whose appearance potential is 20·66 eV

$$CO^+ B^2\Sigma_u^+ + e \rightarrow C^+ {}^2P_{\frac{1}{2}} + O^- {}^2P, \tag{62}$$

or indeed for the appearance of many fragment ions by trapped parent ion processes of a similar nature. Our figure 4 (f) shows clearly the production of C^+ at electron energies well below 20·9 eV, whatever method of calibrating the energy scale is chosen; the electron current densities used in the present experiment are actually lower than those used in many appearance potential studies; so that a critical analysis of the contribution of electron-ion processes to much published fragment ion appearance potential work is indicated, even though positive or zero V_R has always been used in such work. Although the present data has all been collected at negative V_R, our positive repeller peak in Xe has been cursorily studied, and shown to arise from ion trapping. Thus a positive V_R is not a sure protection against trapping, although the condition (see equation (8)) $V = Ka^2 > \frac{3}{2}kT$ is mandatory. An experimental test is the dependence of the fragmentation function on electron current density; the high power of the two electron process dependence makes it possible either to emphasize it or to remove it entirely.

Discrepancies exist in the mass spectrometry of methane; for example, the appearance potentials of fragment ions CH_2^+, CH^+, C^+, do not correspond to the values expected from measurements of the ionization potentials of the radicals CH_2, CH, C. The $I(CH_2^+)$ function is well known to have a form similar to that of C^+ from CO, the data of McDowell & Warren (1951) being reproduced as inset to figure 4 ($g1$), in which the present data are shown. Since we find that CH_2^+ and CH^+ (figure 4 ($g2$)) appear at almost the same potential as CH_4^+, but that the functions below the break at 23 eV are strongly dependent on electron current, some published CH_2^+ and CH^+ fragment ion appearance potentials are in our opinion open to interference from ion-trap effects. The electron energy distribution in the present experiment does not yet enable us to fix an appearance potential to within ± 1 eV. The mass spectra present in our CH_4 experiment showed a variety of gases to be present, in partial pressures deduced to be as follows:

CH_4, $3{\cdot}3\times10^{-9}$ torr; CO, $4{\cdot}8\times10^{-9}$ torr; Ne, $8{\cdot}2\times10^{-7}$ torr;

Kr, $3{\cdot}8\times10^{-8}$ torr; H_2, $6{\cdot}1\times10^{-8}$ torr; Ar, $3{\cdot}5\times10^{-7}$ torr.

But it is unlikely that much interference from such impurities will be experienced at these pressures. Owing to the presence of residual CO, examination of C^+ from CH_4 has not yet proved possible.

6. Future potential of the ion trap

Several fruitful lines of ionic collision study are opened up by the possibility of trapping ions in electron beams.

The limitations of the present experiments must be overcome; outstanding are the inability to measure cross sections absolutely and the difficulties of experimenting at electron energies in excess of that for the direct process of formation of doubly charged ions.

The quality of the trap must be improved, by elimination of electric fields transverse and longitudinal to the electron beam (e.g. by fine mesh grids over the slits), by routine geometrical refinement, by intensifying the beam to deepen the potential well, and by current scaling procedures. Pulsed extraction techniques would facilitate the maintenance of zero transverse field. Under such conditions the yields of ions formed in sequential processes would be improved, and attempts could be made to obtain a trap of constant efficiency, allowing absolute cross sections to be inferred. The use of buffer gases to assist in these attempts is helpful, but not essential. The lowest pressure range might well prove more successful.

Pulse techniques would be necessary for the development of experiments at higher electron energies. Suppose that a low energy beam is passed through a gas, so that only single ionization is possible. A pulse of higher voltage is then applied, so that an ion pulse arising from both single and double processes can be measured. The beam is now switched off for sufficient time for the trapped ions to disperse, and the higher voltage pulse repeated; this time only the single process is possible. By phase sensitive detection the difference signal between the two higher voltage pulses is measured, yielding only the ions formed in the double process.

Such a technique would have the advantage over crossed ion-electron beam techniques using conventional ion sources that by suitable electron energy control only ground state singly charged ions might be studied.

The most valuable application of the ion trap will probably be in appearance potential studies of molecules; not only the critical re-examination of existing electron-molecule experiments, but also in the measurement of appearance potentials arising from electron and photon collisions with molecular ions. Therefore the electron energy distribution must be improved.

Apart from ionization by electrons the ion trap provides a convenient technique for the investigating of the excitation of positive ions by electrons and for the maintenance of ion populations for use in positive ion lasers. Pulse techniques would enable electron energy losses in excitation processes to be investigated. One can also envisage the trapping of negative ions or of electrons in the intense ion beams provided by isotope separators, with consequent possibilities of collision study.

We wish to express our sincere thanks to Professor M. Servigné, who has encouraged this work and provided part of the financial support on behalf of L'Air Liquide, Paris.

The excellent technical assistance of M. D. Joyeux and Mlle. I. Mueller of Institut Battelle has made possible an intensive programme of data accumulation.

Mr L. Moore of University College London is responsible for the integrations leading to equations (7), (17), and (22).

PHILOSOPHICAL TRANSACTIONS OF THE ROYAL SOCIETY A MATHEMATICAL, PHYSICAL & ENGINEERING SCIENCES

Messrs A.E.I., the British manufacturers of the mass-spectrometer used in these experiments, have been extremely helpful at all times.

Dr Lloyd of A.E.R.E. Harwell has discussed the ion trap with us and in particular furnished us with equation (9).

Professor Sir Harrie Massey, F.R.S., has allowed one of us (J. B. H.) considerable latitude to pursue these studies on leave of absence.

References

Bates, D. R. & Moiseiwitsch, B. L. 1954 *Proc. Phys. Soc.* A **67**, 805.
Bleakney, W. 1929 *Phys. Rev.* **34**, 157.
Bleakney, W. 1932 *Phys. Rev.* **40**, 496.
Burgess, A. 1961 *Mém. Soc. Sci. Liege*, **4**, 299.
Daly, N. R. 1965 *Proc. Phys. Soc.* **85**, 897.
Dolder, K. T., Harrison, M. F. A. & Thonemann, P. C. 1961 *Proc. Roy. Soc.* A **264**, 367.
Dolder, K. T., Harrison, M. F. A. & Thonemann, P. C. 1963 *Proc. Roy. Soc.* A **274**, 546.
Dorman, F. H. & Morrison, J. D. 1961 *Canad. J. Phys.* **35**, 575.
Drawin, E. E. 1961 *Zeit. Phys.* **164**, 513.
Fox, R. E. 1960 *J. Chem. Phys.* **33**, 20.
Hagstrum, H. D. 1951 *Rev. Mod. Phys.* **23**, 185.
Hagstrum, H. D. 1956 *Phys. Rev.* **104**, 309.
Hartnagel, H. 1965 *Electronics* **18**, 431.
Hasted, J. B., Lee, A. R. & Hussain, M. 1963 *Proc. 3rd Int. Conf. Electronic and Atomic Collisions London.* Amsterdam: N. Holland Publishing Co.
Hickam, W. M. & Fox, R. E. 1954 *J. Chem. Phys.* **22**, 2059.
Hipple, J. A., Fox, R. E. & Condon, E. V. 1946 *Phys. Rev.* **69**, 347.
Huffman, R. E., Tanaka, Y. & Larrabee, J. C. 1963 *Appl. Optics* **2**, 947; and *J. Chem. Phys.* **39**, 902.
Kupriyanov, S. E. & Latypov, Z. Z. 1963 *J. Expt. Theor. Phys.* **45**, 815: *Soviet Phys. JETP* **18**, 558.
Latypov, Z. Z., Kupriyanov, S. E. & Tunitskii, N. N. 1964 *J. Expt. Theor. Phys.* **46**, 833.
Lloyd, O. 1965 A.E.R.E Harwell. Private communication.
McDowell, C. A. & Warren, J. W. 1951 *Disc. Faraday Soc.* **10**, 53.
McGowan, W. & Kerwin, L. 1962 *Canad. J. Phys.* **38**, 642.
Nier, A. O. 1940 *Rev. Sci. Instrum.* **11**, 212.
Nier, A. O. 1947 *Rev. Sci. Instrum.* **18**, 398.
Petermann, L. A. & Baker, F. A. 1965 *Brit. J. Appl. Phys.* **16**, 487.
Pierce, J. R. 1949 *Theory and design of electron beams.* New York: van Nostrand Co.

PHILOSOPHICAL TRANSACTIONS OF THE ROYAL SOCIETY A MATHEMATICAL, PHYSICAL & ENGINEERING SCIENCES